

## Linking morphodynamic response with sediment mass balance on the Colorado River in Marble Canyon: Issues of scale, geomorphic setting, and sampling design

Paul E. Grams,<sup>1</sup> David J. Topping,<sup>1</sup> John C. Schmidt,<sup>1</sup> Joseph E. Hazel Jr.,<sup>2</sup> and Matt Kaplinski<sup>2</sup>

Received 17 August 2012; revised 17 February 2013; accepted 19 February 2013; published 4 April 2013.

[1] Measurements of morphologic change are often used to infer sediment mass balance. Such measurements may, however, result in gross errors when morphologic changes over short reaches are extrapolated to predict changes in sediment mass balance for long river segments. This issue is investigated by examination of morphologic change and sediment influx and efflux for a 100 km segment of the Colorado River in Grand Canyon, Arizona. For each of four monitoring intervals within a 7 year study period, the direction of sand-storage response within short morphologic monitoring reaches was consistent with the flux-based sand mass balance. Both budgeting methods indicate that sand storage was stable or increased during the 7 year period. Extrapolation of the morphologic measurements outside the monitoring reaches does not, however, provide a reasonable estimate of the magnitude of sand-storage change for the 100 km study area. Extrapolation results in large errors, because there is large local variation in site behavior driven by interactions between the flow and local bed topography. During the same flow regime and reach-average sediment supply, some locations accumulate sand while others evacuate sand. The interaction of local hydraulics with local channel geometry exerts more control on local morphodynamic response than sand supply over an encompassing river segment. Changes in the upstream supply of sand modify bed responses but typically do not completely offset the effect of local hydraulics. Thus, accurate sediment budgets for long river segments inferred from reach-scale morphologic measurements must incorporate the effect of local hydraulics in a sampling design or avoid extrapolation altogether.

**Citation:** Grams, P. E., D. J. Topping, J. C. Schmidt, J. E. Hazel Jr., and M. Kaplinski (2013), Linking morphodynamic response with sediment mass balance on the Colorado River in Marble Canyon: Issues of scale, geomorphic setting, and sampling design, *J. Geophys. Res. Earth Surf.*, 118, 361–381, doi:10.1002/jgrf.20050.

### 1. Introduction

[2] Sediment budgets are one of the most powerful and frequently used conceptual frameworks in fluvial geomorphology. Sediment budgets have been used to evaluate the effects of streamflow regulation [Andrews, 1986], design and evaluate stream restoration projects [Merz *et al.*, 2006; Erwin *et al.*, 2012], and anticipate outcomes following dam removal [Doyle *et al.*, 2003]. The power of the sediment

budget is in the explicit coupling between sediment flux and sediment storage, as described in the general form of the Exner equation for bed-sediment conservation [e.g., Paola and Voller, 2005, equation 20]

$$\frac{\partial \eta}{\partial t} = -\frac{1}{(1 - \lambda_p)} \left( \frac{\partial V_s}{\partial t} + \nabla \cdot Q_s \right) \quad (1)$$

where  $\eta$  is river bed surface elevation,  $t$  is time,  $\lambda_p$  is the bed-sediment porosity,  $V_s$  is the volumetric concentration of sediment in suspension, and  $Q_s$  is sediment flux. Integrating over a river segment and neglecting the term for the time rate of change of sediment in suspension [e.g., Rubin and Hunter, 1982], equation (1) is often expressed in difference form as

$$\Delta S = I - O \quad (2)$$

where  $\Delta S$  is change in sediment storage, and  $I$  and  $O$  are sediment influx and efflux, respectively, for a specified river segment and time interval. We present both equations (1) and (2) to emphasize that the more commonly used difference form (equation (2)) involves integrating both in space and time. In this paper, we explore how the spatial and

<sup>1</sup>U.S. Geological Survey, Southwest Biological Science Center, Grand Canyon Monitoring and Research Center, Flagstaff, Arizona, USA.

<sup>2</sup>School of Earth Sciences and Environmental Sustainability, Northern Arizona University, Flagstaff, Arizona, USA.

Corresponding author: P. E. Grams, U.S. Geological Survey, Grand Canyon Monitoring and Research Center, 2255 N. Gemini Dr., Flagstaff, AZ 86001, USA. (pgrams@usgs.gov)

©2013. The Authors.

This is an open access article under the terms of the Creative Commons Attribution-NonCommercial-NoDerivs License, which permits use and distribution in any medium, provided the original work is properly cited, the use is non-commercial and no modifications or adaptations are made. 2169-9003/13/10.1002/jgrf.20050

temporal scales over which equation (1) is integrated affect the outcome of the mass-balance computation. Using equation (2), measurements or estimates of sediment flux may be used to calculate  $\Delta S$ , ultimately leading to a prediction of equilibrium, or perturbation into surplus or deficit. Alternatively, repeat measurements of channel morphology may be used to calculate  $\Delta S$  and make inferences about changes in sediment flux or watershed sediment supply. Either approach involves a set of assumptions and associated sources of uncertainty, which are discussed further below. If all terms of equation (2) are measured (sediment influx, sediment efflux, and morphologic change), it is possible to test these underlying assumptions and the validity of the computed sediment budget [e.g., *Erwin et al.*, 2012]. In this paper, we present and compare sediment budgets in which all budget terms are measured or estimated for 100 km of the Colorado River in Marble Canyon within Grand Canyon National Park. Because the objectives of this study require tracking the sediment budget over this entire river segment, channel morphologic change was determined from measurements made in selected monitoring reaches. We discuss the physical processes that contribute uncertainty to each budget component, with emphasis on how the spatial distribution of morphologic changes affects attempts to infer segment-scale (~30 km)  $\Delta S$  based on extrapolation of reach-scale (~3 to 5 km) measurements of morphologic change. Extrapolation is typically required wherever study segments are long and measurements of the entire study area are not possible. The insights afforded by our analysis of spatially and temporally extensive data provide guidance in the application of sediment budgets to other situations where less data may be available.

[3] The creation and maintenance of alluvial sandbars is a primary goal of managers of the Colorado River in Grand Canyon National Park. This resource interest has inspired scientists to estimate sediment budgets for the Colorado River since the early 1970s, about 10 years after the completion of Glen Canyon Dam, which is 25 km upstream from the park. Estimates of the sediment budget have ranged from the prediction of severe sediment deficit [*Laursen et al.*, 1976] to the prediction of approximate balance or surplus [*Howard and Dolan*, 1981; *Andrews*, 1991; *U.S. Department of the Interior*, 1995]. The most recent analysis of the post-dam sediment budget indicates that the uncertainty in the sand mass balance is often larger than the difference between influx and efflux [*Topping et al.*, 2000a]. This suggests that the sand budget for much of the Colorado River in Grand Canyon is essentially indeterminate over multi-year time scales. Sand accumulation may occur in years with average or larger tributary inputs and average or lower dam release volumes, but sand depletion is likely in other years and over timescales in excess of decades [*Topping et al.*, 2010a].

[4] The pursuit of sandbar maintenance objectives requires knowledge of sand influx and tracking the changes in sand storage, because Glen Canyon Dam severely limits the supply of sand to Grand Canyon [*Howard and Dolan*, 1981; *Topping et al.*, 2000a]. Previous studies have demonstrated that controlled floods, released from Glen Canyon Dam as experiments, effectively build sandbars along the channel margins [*Hazel et al.*, 1999; *Schmidt et al.*, 1999; *Topping et al.*, 2006a; *Hazel et al.*, 2010]. However, it remains unclear whether the supply of sand provided by tributaries alone is sufficient to support the continued use of controlled floods to

build sandbars with equal effectiveness [*Wright et al.*, 2008; *Schmidt and Grams*, 2011; *Wright and Kennedy*, 2011]. It is possible that continued controlled floods will cause progressive depletion of sediment from storage in the river channel and result in a diminishing capacity for rebuilding sandbars. For these reasons, sand budgets for the Colorado River are constructed by measurements of sand flux at select gages and by repeat measurements of bed morphology.

## 2. Uncertainty and Bias in Sediment Budget Computations

### 2.1. Uncertainty in Flux-Based Sediment Budgets

[5] The most significant source of uncertainty in sediment budgets determined from measurements of sediment flux arises from the potential for undetected persistent biases (systematic error) in either the transport measurements or the computation of flux (the product of discharge and the velocity-weighted suspended-sediment concentration in a cross-section) from those measurements. Whereas random measurement errors will average out with a sufficient number of observations, biases will accumulate and may cause very large systematic errors in computations of flux over longer timescales. Some sources of bias are known and may, therefore, be reduced or eliminated. For example, hysteresis in sediment transport during the passage of a flood is a potential source of systematic error. If hysteresis is undetected or ignored and sediment flux is calculated using a sediment rating curve, estimates of sediment flux and consequent sediment budgets may have an extremely large error [*Gray and Simoes*, 2008]. This type of bias can be reduced by the institution of more frequent sampling such that fluxes may be calculated by interpolating between transport measurements, obviating the need to use a sediment rating curve.

[6] But even with high-resolution measurements of sediment transport, there is potential for undetected persistent biases. These biases may result from unknown sampling problems, problems associated with the measurement site, or persistent bias in the discharge measurements. For example, even published U.S. Geological Survey streamflow records that are labeled “excellent” may have up to 5% uncertainties, and that uncertainty may include a persistent bias [*Rantz et al.*, 1982]. Five-percent-level biases can easily be introduced into transport measurements through non-isokinetic suspended-sediment sampling [*Sabol and Topping*, 2013], poor selection of the sampling cross-section, or an insufficient number of verticals in the cross-section (*Edwards and Glysson*, 1999). Five-percent-level biases can be introduced in discharge measurements made with mechanical current meters through inappropriate characterization of near-bank velocities or the shape of velocity profiles [*Rantz et al.*, 1982], and biases can be introduced into discharge measurements made with acoustic-Doppler current profilers through application of incorrect edge coefficients, extrapolation of the measured velocity profiles to the bed or water surface, or incorrect compensation of moving-bed effects [*Mueller and Wagner*, 2009].

[7] Because these sources of bias can remain undetected and, therefore, persist over long timescales, they will result in systematic error in the computed sediment flux that accumulates over time. Therefore, the uncertainty arising from these potential persistent biases accumulates in the computation of a sediment budget in proportion to the total sediment

flux. Thus, for flux-based change in storage  $\Delta S_f$  calculated from equation (2), the uncertainty over time  $t$  is

$$\Delta S'_f = \sum_t I' + \sum_t O' \quad (3)$$

where the primes denote uncertainty in the respective terms due to potential persistent bias. When sediment budgets are calculated with the recognition that persistent bias may exist, the uncertainty as a proportion of the divergence in the flux can become very large. *Parker* [1988] demonstrated that uncertainty in a sediment budget for the Missouri River, which has a relatively good sediment record, was more than double the difference in sediment load between measurement stations when  $\Delta S$  was not large. Similarly, *Grams and Schmidt* [2005] reported that uncertainty in the estimates of sediment flux on the Green River in Colorado and Utah precluded determination of the sign of the sediment budget.

## 2.2. Uncertainty in Morphologic Sediment Budgets

[8] The uncertainties in sediment budgets computed from morphologic measurements may be grouped into categories parallel to those described above for flux-based budgets. These are measurement error, the spatial and temporal propagation of error in budget computations, and physical processes that cause bias when observations are interpolated or extrapolated. The uncertainty resulting from measurement error can vary widely depending on the measurement method. In section 4, we discuss uncertainty specific to the methods we employed and refer the reader to *Lane et al.* [2003] and *Lane and Chandler* [2003] for more general discussions on uncertainty in topographic measurements. Spatial propagation of error is the method by which measurement uncertainty for a specific point, such as an individual grid cell, is accumulated over the area of interest and contributes to error in a sediment budget calculation.

[9] The approach for estimating spatially propagated error varies depending on the spatial scale of interest. Because an increasing number of studies are utilizing high-resolution topographic data for geomorphic monitoring, there has been renewed interest in understanding and quantifying uncertainty in these datasets [e.g., *Brasington et al.*, 2000, 2003; *Lane et al.*, 2003]. Recent advances have focused on quantifying how measurement error and computational method contribute uncertainty to volumes of morphologic change for specific areas of interest [*Wheaton et al.*, 2010]. These methods provide an estimate of the level of confidence in the computed change for each location (i.e., grid cell) in the area of interest. This approach allows for a spatially variable characterization of uncertainty. However, methods that resolve uncertainty at the level of each grid cell are more detailed and possibly more conservative than is required when the primary interest is net change in storage over a large area, because errors in the measured elevation at each grid cell may have a large random component and therefore largely cancel out as the region of interest becomes large.

[10] When computing a morphologic sediment budget, the essential measure of uncertainty is the uncertainty in the computation of the average surface elevation over the region of interest. The net change in storage over a specified area is exactly equivalent to the difference in

average elevation multiplied by the area. Therefore, change in storage over area  $A$ , which in a grid-based calculation, is given by

$$\Delta S_m = A_c \sum_{c=1}^n (Z_{c(2)} - Z_{c(1)}) \quad (4)$$

and is equivalent to

$$\Delta S_m = A(\bar{Z}_{(2)} - \bar{Z}_{(1)}) \quad (5)$$

where  $\Delta S_m$  is the net change in sediment storage computed by morphologic differencing and  $c$  corresponds to  $n$  cells of equal area  $A_c$  and elevation  $Z_{c(1)}$  at time (1) and  $Z_{c(2)}$  at time (2), with overbars indicating spatially averaged elevation for area  $A$ . If the total uncertainty in the measurements of elevation,  $\bar{Z}'_{(1)}$  and  $\bar{Z}'_{(2)}$ , is known and spatially uniform, the uncertainty in the morphologic budget  $\Delta S'_m$  may be expressed as

$$\Delta S'_m = A(\bar{Z}'_{(2)} + \bar{Z}'_{(1)}) \quad (6)$$

[11] This estimate of uncertainty does not rely on any assumption about the nature of the error. If the uncertainties in equation (6) were known to be independent and random, it would be appropriate to propagate the error in quadrature (*Taylor*, 1997). Although a large component of the uncertainties in equation (6) may be random, they may not be fully independent; therefore, we adopt the more conservative approach of using the ordinary sum. The details involved in our estimation of the uncertainty  $\bar{Z}'$  in the measurements used in this study are discussed in section 4.

[12] It is important to note the differences in error propagation between the flux measurements and the morphologic measurements. Uncertainties in measurements of flux increase in proportion to the cumulative sediment flux (equation (3)). Thus, larger fluxes, typically associated with a longer sediment-budget period, result in greater uncertainty. Measurements of topographic change are, however, independent of the total sediment flux. Whether the budget period is short with small cumulative flux or long with large cumulative flux, the uncertainty in the computation of change in storage based on morphologic measurements is based only on the measurement error associated with each of the topographic surfaces per equation (6).

[13] The approach to uncertainty in morphologic budgets outlined above assumes that topographic measurements are made comprehensively over the entire area of interest. However, that is rarely possible. Sediment budgets are often needed for long segments of a river, for which comprehensive measurements of repeat topography are not available. In these cases, computation of change in sediment storage requires some form of interpolation or extrapolation. Sampling schemes commonly involve the selection of representative sampling sites [*Trimble*, 1983] or the use of channel cross-sections spaced at some interval [*Sutherland and Bryan*, 1991; *Reid and Dunne*, 2003; *Grams et al.*, 2007]. The degree to which a sample of measurements of morphologic change represents net changes in sediment storage is dependent on the geomorphic characteristics of the river. For some river systems, such as alluvial rivers with relatively uniform flood plains, patterns of deposition and erosion may be sufficiently

consistent and understood to allow such extrapolation [Marron, 1992; Walling et al., 1998]. However, many rivers have more complicated sediment storage dynamics. For example, in braided gravel-bed rivers, sediment is stored across the width of the braid belt with highly localized areas of active storage [Bridge and Gabel, 1992; Wheaton et al., 2010]. In river channels with pool-riffle sequences, the pools and riffles are locations of concentrated changes in bed elevation and are known to exhibit systematic transfers of sediment from one storage environment to another for different flow regimes [Lisle, 1982; Lisle and Hilton, 1992]. In particular, it is this process of sediment redistribution determined by local hydraulics that must be carefully evaluated when using measurements of morphologic change to infer a sediment budget.

[14] The relative role of sediment supply and local hydraulics in causing channel change has been examined in several studies of scour and fill at streamflow gaging stations [Leopold and Maddock, 1953; Colby, 1964; Jackson and Beschta, 1984; Topping et al., 2000b]. These data have often been used to evaluate long-term trends in sediment storage. However, Colby [1964] concluded that because some channel cross-sections exhibit discharge-dependent patterns of scour and fill, observations from single cross-sections are often poor indicators of sediment storage changes for a reach of channel. One of the most frequently cited examples of this occurrence is for the Colorado River at the Grand Canyon gaging station [Leopold and Maddock, 1953; Brooks, 1958; Colby, 1964; Howard and Dolan, 1981; Topping et al., 2000b]. Topping et al. [2000b] used observations made from the 1940s through the early 1960s to show how the temporal patterns of scour and fill at the Lees Ferry and Grand Canyon gaging stations were largely decoupled from the upstream sediment supply and largely driven by hydraulics. Although changes in sediment supply may affect the precise timing of peak scour and/or fill during the passage of a flood, Topping et al. [2000b] concluded that the primary cause of scour and fill was the interaction of the local hydraulics with the channel geometry.

[15] The relative influence of flow and sediment flux in controlling morphodynamic response may be evaluated with a simple scaling analysis conducted on a simplified one-dimensional form of the Exner equation (equation (1)). First, the term  $\partial V_s/\partial t$  in equation (1) for the time rate of change in sediment concentration in the flow has been shown to be negligible in scaling analyses by Rubin and Hunter [1982] and Paola and Voller [2005]; therefore, the contribution of this term can be ignored. Second, if we assume that bed-sediment porosity is constant, changes in bed elevation are controlled entirely by the remaining term on the right side, which represents the spatial divergence of sediment flux. Third, we can greatly simplify the scaling analysis by making the problem one dimensional by replacing  $Q_s$  with  $q_s$ , the sediment flux per unit width.  $q_s$  is equal to the product of the depth-averaged suspended-sediment concentration  $C_s$ , flow velocity  $U$ , and flow depth  $h$ :

$$q_s \approx C_s U h \quad (7)$$

Thus, the divergence of the sediment flux depends on spatial changes in suspended-sediment concentration, flow velocity, and flow depth. Typical relations for suspended-sediment concentration include parameters for flow strength, sediment grain size, and a measure of sediment

availability. Using the formulation of Rubin and Topping [2001, 2008] and Topping et al. [2010a],

$$C_s \propto u_*^{3.5} D_b^{-2.5} A_s \quad (8)$$

where  $u_*$  is shear velocity (a measure of flow strength),  $D_b$  is the median grain size of the suspendable bed sediment, and  $A_s$  is a fractional measure of the amount of the suspendable sediment covering the bed. Flow strength and grain size are related nonlinearly with concentration while the relation between supply and concentration is linear. Although other measures of sediment supply could be used, we use  $A_s$  as defined above, because the approximately linear relation between this measure of supply and suspended-sand concentration has been demonstrated in laboratory flume experiments [Grams and Wilcock, 2007]. Rewriting equation (1) in one-dimensional difference form where  $X$  is distance in the streamwise direction, removing the negligible influence of  $\partial V_s/\partial t$ , assuming constant bed-sediment porosity, using equation (7) for sediment flux, and equation (8) for sediment concentration, results in the following proportionality:

$$\frac{\Delta \eta}{\Delta t} \propto - \frac{\Delta(u_*^{3.5} D_b^{-2.5} A_s U h)}{\Delta X} \quad (9)$$

Taking  $u_* \propto U$  then results in the simpler proportionality,

$$\frac{\Delta \eta}{\Delta t} \propto - \frac{\Delta(u_*^{4.5} D_b^{-2.5} A_s h)}{\Delta X} \quad (10)$$

[16] Because  $\eta$  is positive upward, deposition occurs when there is a spatial decrease in flow strength, increase in bed-sand grain size, or decrease in bed-sand cover. Conversely, erosion occurs when there is a spatial increase in flow strength, decrease in bed-sand grain size, or increase in bed-sand cover. The proportionality also demonstrates that the strongly nonlinear relation between flow strength and transport means that spatial variations in flow are a stronger control on erosion and deposition than changes in sediment supply (bed-sand cover). Small spatial changes in flow strength will result in large divergences of the transport leading to rapid changes in bed elevation. Changes in supply are not unimportant but have a weaker effect on transport. For example, in a straight channel with constant roughness, and no divergence in the flow strength (i.e., boundary shear-stress field), changes in bed elevation will result entirely from changes in sediment supply and grain size. This principle is also true for changing discharge so long as channel uniformity is maintained. In these cases, changes in bed elevation likely do indicate changes in sediment supply. However, variations in channel geometry within an otherwise uniform reach result in systematic patterns of scour and fill that are caused by local divergence in the boundary shear-stress field rather than changes in sediment supply to the reach.

[17] This scaling analysis demonstrates that local changes in morphology (i.e., local changes in sediment storage) are most strongly controlled by local hydraulics. It is also required that over the length of a river segment, net changes in storage are determined by the difference between the sediment supply and the sediment export. At some spatial scale, local processes

must become averaged such that  $\Delta S_m = \Delta S_f$ . However, while many studies have shown that local changes in storage may result from local hydraulics rather than changes in the sediment budget, the spatial scale over which these processes dominate is poorly known. Below, we evaluate both the relative magnitude of local changes in sediment storage and the spatial scale at which they dominate the sediment budget.

### 3. Description of Study Area

[18] The combination of high-resolution streamflow and sediment-transport data and well-understood geomorphic characteristics make the Colorado River in Grand Canyon well suited for a field-scale examination of the interactions between sediment supply and local morphodynamic response of the bed. Because the river has long held interest as both a critically important transfer of water supply and as a central focal point of a highly visited national park, the records for both streamflow and sediment transport are exceptionally rich. Measurements for streamflow and suspended-sediment transport date back to the 1920s, with higher quality suspended-sediment data collected at several gages since the late 1940s. Owing to current interest in managing the water and sediment in Grand Canyon, both streamflow and suspended-sediment concentration are now monitored continuously at 15 min intervals at six locations in the 467 km of the Colorado River between Glen Canyon Dam and Lake Mead reservoir (Figure 1).

[19] The large-scale structure of the Colorado River corridor in Grand Canyon is determined by relatively immobile bedrock, talus, and tributary debris fans. However, there is also an adjustable component of channel morphology that is composed of cobbles, gravel, and highly mobile fine

sediment [Howard and Dolan, 1981]. This fine sediment, dominated by sand, forms narrow discontinuous deposits along the channel margins and larger deposits in zones of recirculating flow (eddies) [Howard and Dolan, 1981; Schmidt, 1990]. The ubiquitous bouldery debris fans located at tributary mouths [Dolan et al., 1978] control channel gradient, cause nearly all of the rapids [Howard and Dolan, 1981; Webb et al., 1989], and constrict the channel, resulting in recirculation zones where most sand deposits are found [Schmidt, 1990]. Schmidt and Rubin [1995], therefore classified the Colorado River in Grand Canyon and similar river segments elsewhere as “debris-fan dominated canyons.” Because the sandbars and in-channel fine sediment are mostly sand, that size fraction of the sediment budget is the focus of this study.

[20] Regulation of Colorado River streamflow began when Glen Canyon Dam was completed in March 1963. Since then, the dam and its operations have eliminated annual spring floods, eliminated the upstream supply of sand, and increased the magnitude of base flows [Topping et al., 2000a; Topping et al., 2003]. The mean annual discharge of the Colorado River at Lees Ferry has decreased from a pre-dam average of 470 m<sup>3</sup>/s (water years 1922–1962) to a post-dam average of 376 m<sup>3</sup>/s (water years 1963–2010). This 20% reduction in annual flow is the combined result of upstream consumptive use, reservoir evaporation, and regional decreases in runoff [Woodhouse et al., 2006]. During the May 2002 to May 2009 study period, the mean annual flow was 332 m<sup>3</sup>/s, 12% less than the post-dam average. Under current dam operation guidelines, releases are typically between about 170 and 700 m<sup>3</sup>/s, with daily fluctuations for hydroelectric power generation of 142 to 227 m<sup>3</sup>/s (Figure 2a).

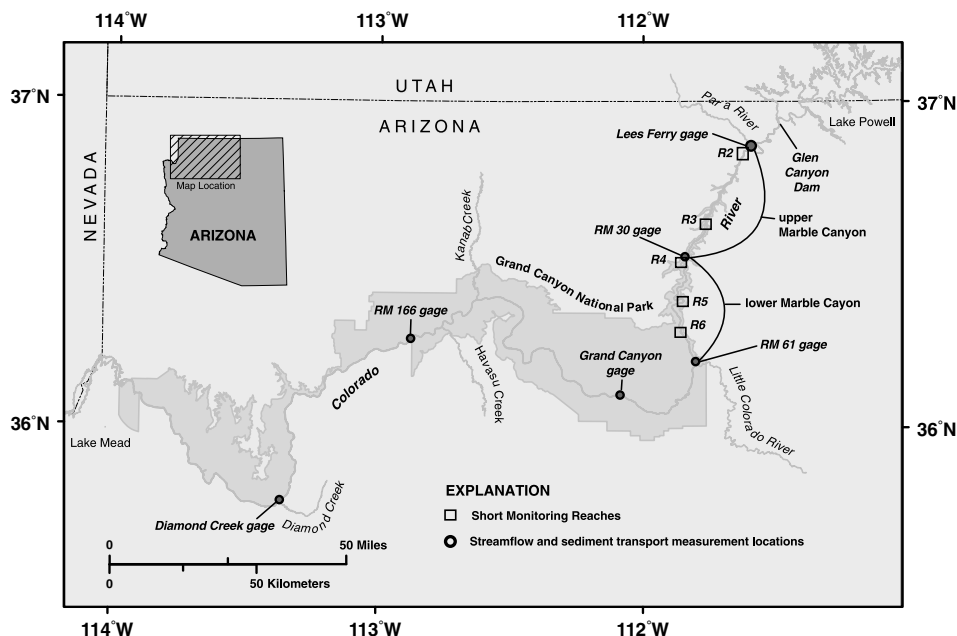


**Figure 1.** Map of the Colorado River from Glen Canyon Dam to Lake Mead, Arizona, showing streamflow and sediment monitoring stations (circles) and the short monitoring reaches where morphologic measurements were made (boxes). The upper Marble Canyon mass-balance segment extends from Lees Ferry to the gage at RM 30. The lower Marble Canyon mass-balance segment extends from the RM 30 gage to the RM 61 gage.

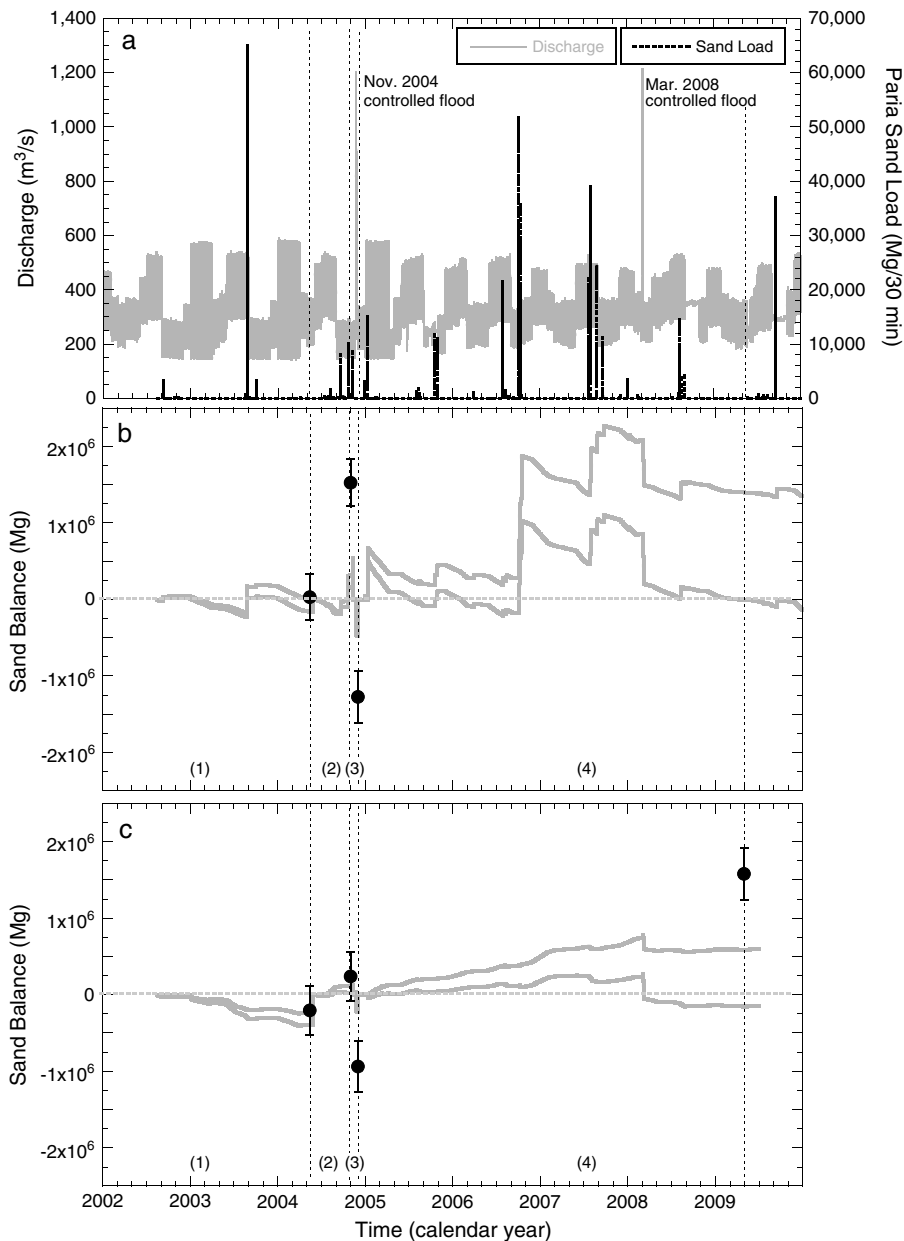


**Figure 2.** Discharge, Paria River sediment input, and changes in sand mass balance. (a) Unit (15 min) discharge for the Colorado River at Lees Ferry in gray and unit (30 min) sand load for the Paria River at Lees Ferry in black. (b) Sand mass balance for upper Marble Canyon (RM 0 to RM 30). The gray lines show the upper and lower uncertainty bounds of the flux-based mass balance; the black points show the morphologic sand storage change extrapolated to the mass-balance segment. The flux-based mass balance begins at zero and is reset to zero immediately following each morphologic measurement. (c) Sand mass balance for lower Marble Canyon (RM 30 to RM 61). The gray lines show the upper and lower uncertainty bounds of the flux-based mass balance; the black points show the morphologic sand storage change extrapolated to the mass-balance segment. The flux-based mass balance begins at zero and is reset to zero immediately following each morphologic measurement. The dashed vertical lines shown in each plot divide the sand budget periods shown in Table 3: (1) May 2002 to May 2004; (2) May 2004 to November 2004; (3) November 2004 to December 2004; and (4) December 2004 to May 2009.

[21] The focus of this study is the segment of the Colorado River between the Paria River confluence at Lees Ferry (25 km downstream from Glen Canyon Dam) and the Little Colorado River confluence, 98 km downstream from Lees Ferry (Figure 1). This part of Grand Canyon is known as Marble Canyon, which for the purpose of sand budgeting,

we informally divide into upper Marble Canyon and lower Marble Canyon. Throughout Marble Canyon, debris fans, large rapids, and recirculating eddies are common. Upper Marble Canyon is narrower than lower Marble Canyon and has a lower frequency of eddies and associated sandbars [Schmidt and Graf, 1990; Hazel et al., 2006]. We refer to

these two parts of Marble Canyon as mass-balance segments. Streamflow and sand flux have been measured at 15 min intervals at the upstream and downstream boundaries of each segment since August 2002.

[22] Five short study reaches were established in Marble Canyon for the purpose of monitoring long-term changes in sand storage. We refer to these as the “short” monitoring reaches to distinguish them from the much longer mass-balance segments. Each reach is approximately 3 to 5 km in length and includes 11–25 eddy depositional zones (EDZs), each occurring in the lee of a debris fan (Table 1). The short reaches differ in the type of bedrock that occurs at river level, the frequency of debris fans, the average size of EDZs, average width, and gradient (Table 1). Short monitoring reaches R2 and R3 are in upper Marble Canyon and begin at river mile (RM) 1 and 22, respectively (locations along the Colorado River in Grand Canyon are referenced by the convention of river mile, which is the distance downstream from Lees Ferry along the channel centerline). Short monitoring reaches R4, R5, and R6 are in lower Marble Canyon and begin at RM 29, 43, and 54, respectively.

## 4. Methods

### 4.1. Mass Balance From Measured Sand Flux

[23] A network of continuously operating streamflow and suspended-sediment monitoring stations was established on the Colorado River in Grand Canyon to track both the accumulation of tributary sand inputs and the downstream redistribution of those inputs in the channel [Topping *et al.*, 2010b; Griffiths *et al.*, 2012]. These stations are located at approximately 50 to 130 km intervals (Figure 1) and include instruments for measuring water stage (to determine discharge) and a combination of side-looking acoustic and laser-diffraction instruments that are used to make surrogate measurements of suspended-sand concentration and grain size at 15 min intervals [Topping *et al.*, 2006b, 2007, 2010b; Wright *et al.*, 2010a, 2010b]. The data collected by the sediment-surrogate instruments were calibrated and subsequently verified using conventional measurements of suspended-sediment concentration and grain size collected during periodic sampling. Stage was converted to discharge using the standard USGS methods described in Rantz *et al.* [1982]; 15 min instantaneous sand loads were calculated as the product of the 15 min sand-concentration measurements and computed discharges [Porterfield, 1972]; cumulative sand loads were then calculated by integrating the 15 min instantaneous loads

[Porterfield, 1972]. Based on measurements by Rubin *et al.* [2001], sand loads were increased by 5% at each station to account for bedload and unmeasured suspended load in the zone near the bed not sampled by depth-integrating samplers. Together with measured sand loads from gaged major tributaries and small estimated loads from ungaged tributaries, differences in the cumulative load between stations were used to calculate the sand mass balance, or flux-based sand storage change  $\Delta S_F$ , for each mass-balance segment (Figure 2). For comparison with the morphologic measurements of sand storage change, we computed mass balances for each time interval between the topographic/bathymetric surveys.

[24] Uncertainties in the computed mass balances largely result from potential biases in the conventional measurements of suspended-sand concentration, the calibrations between the conventional samples and the surrogate instruments, the estimates from tributary inputs, and the streamflow measurements. Considering the relative importance of all of these sources of uncertainty, Topping *et al.* [2010a] assigned uncertainties of 5, 10, and 50% to the sand loads on the main-stem gages, tributary gages, and ungaged tributaries, respectively. Because these uncertainties represent the potential maximum magnitudes of persistent biases that are believed to possibly exist in the measurements, these uncertainties accumulate over time as per equation (3). Thus, when the budget is calculated for longer time periods with greater cumulative loads, there is larger uncertainty. Moreover, because these uncertainties largely arise from potential biases with unknown probabilities of occurrence, they cannot be treated as random. That means there is no greater likelihood that the actual mass balance is in the center of the uncertainty range than near the margins; the actual value could have equal probability of occurring anywhere in the range of uncertainty. Over long timescales (depending on the magnitude and source of the loads), the accumulating uncertainty in the sand mass balance eventually becomes larger than the differences in the sand mass balance between gages, resulting in an indeterminate sand budget, thus the value of direct measurements of change in storage by morphologic methods increases.

### 4.2. Sand Storage Change From Morphologic Measurements

[25] The topography and bathymetry of each study reach were measured by a combination of ground-based survey, airborne remote sensing, and boat-based sonar. The short monitoring reaches were surveyed in May 2002, June 2004, November 2004, and December 2004. In April 2009, the three

**Table 1.** Summary Characteristics of Mass-Balance Segments and Short Monitoring Reaches in Marble Canyon

| Mass-Balance Segment | Short Monitoring Reach | Extent (RM)  | Length (km) | Average Channel Width (m) | Water Surface Slope | Number of Large EDZs <sup>a</sup> | Average size of Large EDZs (m <sup>2</sup> ) |
|----------------------|------------------------|--------------|-------------|---------------------------|---------------------|-----------------------------------|--|
| Upper Marble Canyon  |                        | 0.0 to 29.4  | 48.3        | 79                        | 0.0014              | NA <sup>b</sup>                   | NA   |
|                      | R2                     | 1.1 to 2.8   | 2.7         | 116                       | 0.0002              | 11                                | 4,300  |
|                      | R3                     | 21.9 to 23.6 | 2.7         | 66                        | 0.0016              | 25                                | 3,900  |
| Lower Marble Canyon  |                        | 29.4 to 61.0 | 49.9        | 94                        | 0.0010              | NA                                | NA   |
|                      | R4                     | 29.4 to 32.0 | 4.2         | 74                        | 0.0009              | 23                                | 3,000  |
|                      | R5                     | 42.5 to 45.4 | 4.7         | 100                       | 0.0009              | 21                                | 11,000                                       |
|                      | R6                     | 54.4 to 56.1 | 2.7         | 111                       | 0.0003              | 24                                | 4,300  |

<sup>a</sup>Eddy depositional zones that contain sandbars.

<sup>b</sup>No data available.

short monitoring reaches in lower Marble Canyon (R4, R5, and R6) were surveyed as part of a campaign to map the entire mass-balance segment between RM 30 and RM 61. Multibeam sonar was used to map as much of each reach as possible, but rapids and areas along the shoreline where depths were less than about 1 m could not be mapped with this method. In each reach, this resulted in the mapping of approximately 80% of the bed. Because the excluded areas are in rapids dominated by coarse material, sand storage changes in the unmapped areas are assumed negligible. Total stations were used to survey the shallow areas along the shorelines too shallow for multibeam sonar. Topography above the water surface was measured with digital aerial photogrammetry in May 2002, airborne LIDAR in 2004, and ground-based electronic total station in 2009. In 2009, singlebeam sonar was used in addition to multibeam sonar to map along the shoreline. The details of the methods used for sonar data collection and processing are described by *Kaplinski et al.* [2009], and the methods for the total station surveys and site positioning are described by *Hazel et al.* [2008].

[26] The data from each method of survey were edited, processed, and checked for errors independently, then combined in a single point file. This point file was used to create a triangular irregular network (TIN) model of the surface for each reach, which was checked for errors and discrepancies among survey methods. The TIN models were used to create 1 m resolution digital elevation models (DEMs) for each survey. The 1 m spatial resolution was chosen as the best compromise between the high point density data generated by multibeam sonar, photogrammetry, and LIDAR (10s to 100s of points/m<sup>2</sup>) and the lower point density data generated by singlebeam sonar and total station survey (<1 point/m<sup>2</sup>). The lower resolution of the total station data is partially compensated by point selection; surveys made use of topographic breaklines, which were used in generating the TIN model. The DEMs for each reach were coregistered such that grid cells for successive surveys were precisely coincident. Changes between surveys were calculated as the difference in elevation for corresponding grid cells to produce grids depicting areas of erosion and deposition, which we refer to as difference maps. Changes in storage were computed only for the region common to all surveys. Areas thus excluded were typically above the level inundated during the study period. The difference maps and calculations of changes in sediment storage volume were performed in ArcGIS.

[27] Because our primary interest is net change in sediment storage  $\Delta S$  over each short monitoring reach, we base our estimate of uncertainty on the uncertainty associated with determining the average elevation of each surface (equation (6)). This uncertainty could be estimated by combining individual estimates of measurement error, positioning error, interpolation error, etc. An alternative approach is to estimate total uncertainty by evaluation of repeat surveys for selected areas in the channel identified to be stable over time. Because this approach is based on comparisons of the final topographic surfaces, it incorporates both random error and bias. For this analysis, 17 areas within the three reaches monitored for the entire 2002–2009 study period were selected. These are areas that are at least 100 m<sup>2</sup> in area, have coarse (gravel or coarser) bed material, and are relatively flat. These areas include cobble bars, areas of talus blocks, and some areas of bedrock outcrop. By visual inspection, all of

these “fiducial” [*sensu Brock et al.*, 2001] areas appear stable over the course of the study period. For each fiducial area, we computed the mean elevation for each survey. Because these are bathymetric measurements, we do not have an independent measure of elevation for the fiducial areas. We, therefore, used the mean value among the mean elevations for the individual surveys as an estimate of the “expected” elevation. For each fiducial area and each survey, we calculated the fiducial polygon error as the difference between the observed mean elevation and the expected mean elevation for that polygon. Combining the 17 fiducial polygons among the three reaches and all available surveys resulted in 101 comparisons.

[28] The distribution of the fiducial polygon errors is slightly left skewed with a median of  $-0.01$  m and a mean value of  $0.00$  m (Figure 3). This suggests that the total uncertainty in our topographic surfaces may be treated as a Gaussian distribution. Because we are interested in potential bias, it is necessary to use the absolute values of the fiducial polygon errors to calculate the uncertainty associated with the repeat bathymetric surveys. This potential bias was calculated as the mean absolute error of all fiducial polygons and is  $0.045$  m, with standard deviation of  $0.058$  m. For a Gaussian normal error distribution, the standard error (68% confidence error) is 1.25 times the mean absolute error, or  $0.056$  m. In other words, the average elevation of a fiducial polygon for a given survey is expected to be within  $0.06$  m of the average elevation of the same area for any other survey with a 68% level of confidence. We apply this uncertainty estimate uniformly to the entire survey area including the areas mapped by other methods, because they have equal or smaller uncertainty [*Hazel et al.*, 2008] and occupy a relatively small proportion of the total survey area.

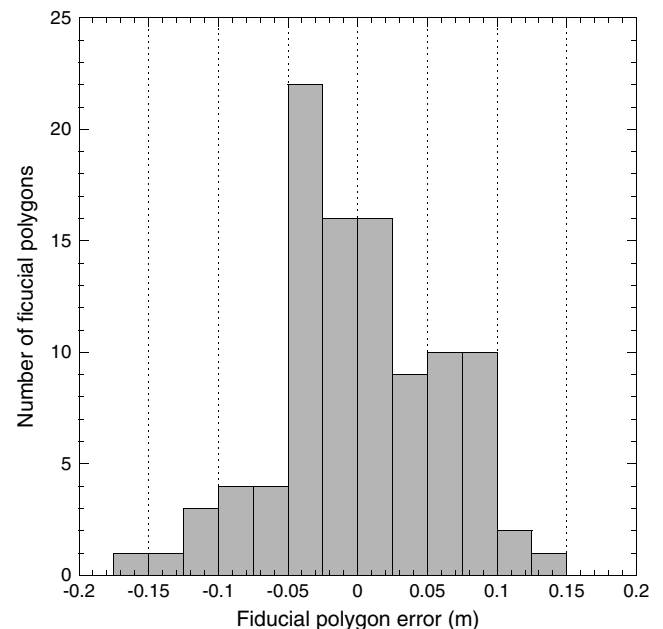


**Figure 3.** Histogram showing fiducial polygon error. Fiducial polygons are areas of the bed that were assumed to be stable for the period of study. The fiducial polygon error is the difference in average elevation for a fiducial polygon between an individual survey and the average among all surveys.

Volumetric changes resulting from topographic differencing were converted to changes in mass using a sediment density of  $2650 \text{ kg/m}^3$  and an assumed deposit porosity of 40% for well-sorted submerged sand [Curry *et al.*, 2004].

[29] Because the focus of this study is on the sand fraction of the sediment budget, it is necessary to estimate the fraction of the morphologic changes that are sand and the fraction that are coarser than sand. We created a higher resolution DEM (25 cm) for the areas of the channel mapped by multibeam sonar and used this and observations of the bed made by underwater video camera to estimate the fraction of the bed covered by sand and the minimum proportion of volume change that is likely sand. We assume that areas of the bed not mapped by multibeam sonar (except rapids and riffles) have the same proportion of sand as the areas that were mapped. This assumption, while possibly not exactly correct, is justified for two primary reasons. First, the majority of the study area was mapped by multibeam—on average 18% of each reach was mapped by other methods. Secondly, the areas that were mapped by other methods, while closer to the shoreline, are not systematically different—that is gravel bars or areas adjacent to debris fans were not preferentially mapped by a different method.

[30] The underwater video camera was used to measure the sand grain size [Rubin *et al.*, 2007] and to distinguish sand from coarse substrate. Observations were made at the time of each of the 2002 and 2004 surveys. The camera was lowered to the bed of the river for a point observation of bed texture at one to five locations across the channel on transects spaced 50 to 200 m apart. On average, approximately 70 observations were made per kilometer within each monitoring reach during each survey.

[31] The 25 cm DEMs were classified into areas that are topographically smooth and topographically rough by analysis of the variation in light intensity between adjacent pixels. Pixel intensity was classified using the ArcGIS hillshade routine with 90-degree (overhead) illumination angle. For each cell, the focal standard deviation of the intensity was calculated for a nine-cell ( $0.56 \text{ m}^2$ ) moving window. Cells with a focal standard deviation less than a specified threshold were classified as smooth. Cells exceeding the threshold were classified as rough. The results from the automated classification were aggregated into polygons with a minimum polygon area of  $25 \text{ m}^2$  (Figure 4). The classified polygons were visually inspected and compared with the underwater video camera observations. This process was repeated until it was found that the threshold focal standard deviation value of 10 provided the best agreement between observed and classified bed texture. Areas of the bed covered by dunes presented a challenge to the automated classification method. These were often classified as rough surfaces, whereas the objective of the classification was to discriminate sand and finer sediment from coarser sediment. These areas were reclassified as sand by visual inspection.

[32] The changes in sand storage computed from repeat topographic/bathymetric surveys for the short monitoring reaches were compared with the changes in sand storage based on the difference between sand influx and sand efflux for the long mass-balance segments by extrapolating the morphologic measurements to the rest of each mass-balance segment outside the monitoring reaches. Extrapolation from the short monitoring reaches required several assumptions about the

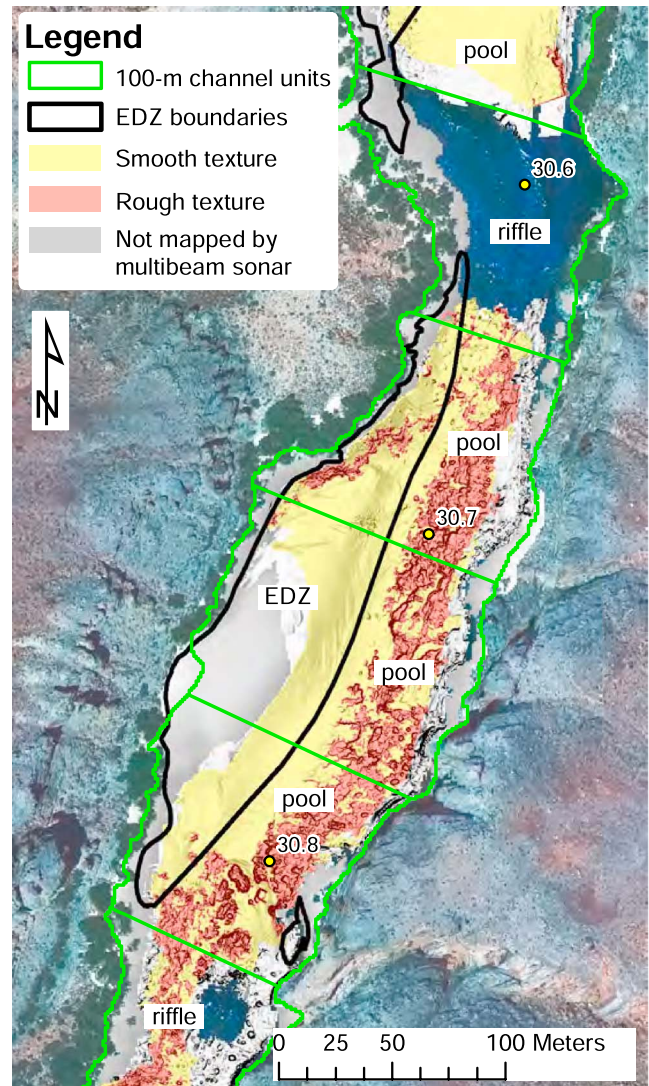


**Figure 4.** Map showing a 0.5 km portion of short monitoring reach R4. Portions of the channel mapped by multibeam sonar and classified as texturally smooth are shown in yellow hillshade. Areas classified as rough are shown in red hillshade. Areas shaded gray were mapped either by total station survey, LIDAR, or photogrammetry. The EDZ for this eddy is shown as the thick black line. Note the topographic break between the sandbar and the river channel. The green lines show the 100 m pool and riffle channel units within the channel area inundated at a discharge of  $1274 \text{ m}^3/\text{s}$ . Direction of streamflow is from north to south.

distribution of sediment storage changes. First, we assumed that all changes within each short monitoring reach occurred within the area mapped and that changes outside the mapped area were negligible. In each survey, the majority of each reach was mapped, and most areas not mapped consisted largely of relatively immobile material. Thus, this assumption is likely reasonable. Second, we assumed that the storage changes per unit area of channel within the short monitoring reaches were representative of the changes per unit area outside the short monitoring reaches. The storage changes outside the short monitoring reaches were calculated as

$$\Delta S_2 = \frac{\left(\frac{\Delta S_1}{A_1} + \frac{\Delta S_3}{A_3}\right)}{2} A_2 \quad (11)$$

where  $\Delta S_2$  is the extrapolated change in storage for the unmeasured reach (2) between monitoring reaches (1) and (3) with measured storage changes of  $\Delta S_1$  and  $\Delta S_3$ . Reaches (1), (2), and (3) have channel areas  $A_1$ ,  $A_2$ , and  $A_3$ , respectively. For all reaches, channel area was treated as a constant and computed as the area below the stage associated with a discharge of 227 m<sup>3</sup>/s in May 2002 [Magirl *et al.*, 2008]. This measure of channel area does not limit the extent of change to that stage elevation but simply provides a means to scale the computed sand storage changes based on relative channel size. The uncertainty associated with the extrapolation is large and cannot be precisely quantified. For our extrapolated budgets, we use the same uncertainty as was used for the reaches that were mapped. Thus, we report the uncertainty as though there were no extrapolation error. This extrapolation has the embedded assumption that the change in storage scales with channel width and that all geomorphic elements occur in the same frequency in the unmapped areas as in the short monitoring reaches. The assumption of zero extrapolation error is the critical assumption that we evaluate below by comparison between the flux-based mass balance and the morphologic-based estimate of storage change. In essence, the assumption of zero extrapolation error requires that hydraulic controls on sediment erosion and deposition in the reaches not mapped be similar to the reaches mapped.

[33] The changes in sediment storage were examined in detail by two different methods. The first method was based on the channel-organizing framework provided by the debris fan-eddy complexes. Because most of the large exposed sandbars occur in eddies and because the hydraulic characteristics of recirculating eddies clearly distinguish them from the main channel, eddies provide a logical basis for segregating changes in sand storage. The one difficulty lies in defining a single fixed boundary for the eddy, because the locations of flow separation and reattachment vary as a function of discharge [Schmidt, 1990]. A precise definition of the eddy boundary would change with flow, requiring observations of each eddy at a range of flows. While such a definition based on the flow field would be the most hydraulically precise, it would be problematic to implement a variable boundary in an analysis of sediment storage change. Instead, we used a method based on that described by Schmidt *et al.* [2004] and Hazel *et al.* [2006]. Schmidt *et al.* [2004] defined the eddy deposition zone (EDZ) area as the geometric union of all areas within a single debris fan-eddy complex covered by a subaerially exposed sand deposit in available aerial photographs. This method is an objective means of defining the region of potential eddy sandbar deposition. However, this method has the disadvantage of omitting the portions of the eddy occupied by a submerged sandbar. We modified this method by expanding the boundaries of the EDZs used by Schmidt *et al.* [2004] to extend into the channel to the topographically defined base of the eddy sandbar (Figure 4). The break in slope separating the sandbar from the main channel was identified by visual inspection of all of the bathymetric maps used in this study, and using the deposit that projected farthest into the channel to define the boundary.

[34] The second method of examining the details of sand storage changes involved segregation between pool and riffle channel environments. Riffles have relatively steep water surface slope and occur adjacent to debris fans or other channel constrictions and around gravel bars (Figure 4). Pools have a low water surface slope and are typically deeper and wider than riffles. Pools include eddies, the channel adjacent to eddies, and ponded segments of channel upstream from rapids and riffles. For the purpose of segregating sediment storage, pools and riffles were mapped in 100 m channel units. The channel was divided into trapezoidal units 100 m in length along the channel centerline with cross-channel boundaries perpendicular to the centerline (Figure 4). Each 100 m unit was classified as a pool or riffle, based on the dominant feature.

## 5. Results

### 5.1. Bed Texture

[35] The maps of bed texture derived from the multibeam sonar bathymetric data together with the observations made by underwater video camera indicate that a substantial majority of the measured changes in bed-sediment storage consisted of sand. In all of the bed texture maps, material classified as topographically smooth (Figure 4) was most common, and the majority of change in sediment storage volume occurred in those areas (Table 2). A lesser amount of change in sediment volume occurred in areas that were classified as topographically rough.

[36] The textural classifications of smooth and rough were converted to grain-size classifications of sand and coarse material, based on the underwater video camera observations. Of the areas classified as topographically smooth, 71% of the observations by underwater video camera indicated a sand bed. Areas classified as smooth that were not sand consisted of topographically flat gravel-size material. Of the areas classified as topographically rough, 37% of the observations by underwater video camera indicated a sand bed. Sand was typically observed with the underwater video camera in areas classified as rough where there was sand in the interstitial spaces among cobbles and boulders.

[37] We used the above estimated proportions of sand associated with the smooth and rough textural classifications to estimate the weighted proportion of volume change that involved sand for each reach and survey interval. For each difference map, we estimated the proportion of volume change that was sand as

$$\Delta V_{\text{sand}} = \Delta V_{\text{smooth}} F_{\text{ssmooth}} + \Delta V_{\text{rough}} F_{\text{srough}} \quad (12)$$

where  $\Delta V_{\text{sand}}$  is the fraction of total volume change that is sand,  $\Delta V_{\text{smooth}}$  is the fraction of volume change in areas classified as smooth in the second of the two DEMs being compared,  $F_{\text{ssmooth}}$  is the fraction of sand in smooth areas (71%),  $\Delta V_{\text{rough}}$  is the fraction of volume change in areas classified as rough in the second DEM being compared, and  $F_{\text{srough}}$  is the fraction of sand in rough areas (37%). The estimated fraction of volume change that is sand rarely differs by more than 1 or 2% within each reach and ranges from a low of 57% in R3 to a high of 71% in R2 (Table 2). Because this method does not explicitly differentiate between processes of bed elevation change between areas that are

**Table 2.** Abundance of Each Textural Category for Each Survey, the Proportion of Sediment Volume Change Associated With Each Possible Change in Textural Categorization, and the Estimated Proportion of Volume Change That Is Sand

| Reach | Date     | Area With Indicated Texture <sup>a</sup> , % |       | Change in Volume From Previous Date for Indicated Change in Texture, % |                 |                |                 | Volume Change That Is Sand <sup>b</sup> , % |
|-------|----------|--|-------|--|-----------------|----------------|-----------------|---|
|       |          | Smooth                                       | Rough | Smooth-to-Smooth   | Smooth-to-Rough | Rough-to-Rough | Rough-to-Smooth |   |
| R2    | May 2002 | 93   | 7     | –  | –               | –              | –               | –   |
|       | May 2004 | 94   | 6     | 91   | 2               | 5              | 2               | 69  |
|       | Nov 2004 | 96   | 4     | 95   | 0               | 1              | 3               | 71  |
|       | Dec 2004 | 93   | 7     | 94   | 5               | 1              | 0               | 69  |
| R3    | May 2002 | 61   | 39    | –  | –               | –              | –               | –   |
|       | May 2004 | 61   | 39    | 53   | 6               | 36             | 5               | 57  |
|       | Nov 2004 | 59   | 41    | 54   | 6               | 34             | 5               | 57  |
|       | Dec 2004 | 58   | 42    | 67   | 6               | 19             | 7               | 62  |
| R4    | May 2002 | 67   | 33    | –  | –               | –              | –               | –   |
|       | May 2004 | 69   | 31    | 66   | 4               | 24             | 6               | 62  |
|       | Nov 2004 | 71   | 29    | 68   | 4               | 22             | 5               | 62  |
|       | Dec 2004 | 70   | 30    | 80   | 6               | 11             | 4               | 65  |
| R5    | May 2009 | 71   | 29    | 78   | 4               | 10             | 8               | 66  |
|       | May 2002 | 88   | 12    | –  | –               | –              | –               | –   |
|       | May 2004 | 88   | 12    | 89   | 3               | 6              | 2               | 68  |
|       | Nov 2004 | 88   | 12    | 87   | 2               | 8              | 3               | 68  |
| R6    | Dec 2004 | 87   | 13    | 91   | 5               | 2              | 1               | 68  |
|       | May 2009 | 99   | 1     | 88   | 2               | 2              | 8               | 69  |
|       | May 2002 | 88   | 12    | –  | –               | –              | –               | –   |
|       | May 2004 | 88   | 12    | 88   | 3               | 6              | 2               | 68  |
| R6    | Nov 2004 | 90   | 10    | 90   | 1               | 5              | 4               | 69  |
|       | Dec 2004 | 89   | 11    | 92   | 4               | 2              | 2               | 69  |
|       | May 2009 | 89   | 11    | 92   | 2               | 2              | 3               | 69  |

<sup>a</sup>Percent of area mapped by multibeam sonar.<sup>b</sup>See equation (12).

entirely sand and areas that are partially sand, and because it is not possible to verify the composition of the subsurface, we do not have a basis for an estimate of uncertainty. The values reported in Table 2 are, however, likely minimum estimates for the fraction of the total change in storage that involves sand. For example, in areas of the bed classified as rough where we estimate that about 37% of the surface is actually sand, we assume that 37% of the volume change consisted of sand and the remainder of change involved coarser material. It is, however, likely that a greater proportion of the volume change in those areas included sand than included less-mobile coarse sediment. All changes for sand storage reported below are based on the estimated proportions of sand shown in Table 2.

## 5.2. Sediment Budgets for Upper and Lower Marble Canyon

[38] The study period included intervals of both positive and negative net changes in sand storage in Marble Canyon. The change in sand storage based on morphologic differencing in the study reaches ranged between  $-189,000$  Mg ( $-69,000$  Mg/km) to  $231,000$  Mg ( $84,000$  Mg/km). The budget was negative in four out of the five short reaches in the May 2002 to May 2004 period, positive in all reaches between May 2004 and November 2004, negative or near zero in all reaches between November 2004 and December 2004, and positive in all three lower Marble Canyon reaches between December 2004 and May 2009 (Table 3). The sign of these morphologic budgets is consistent with the sign of

**Table 3.** Morphologic and Flux-Based Sand Budgets

| Reach   | May 2002–May 2004 |                        | May 2004–Nov 2004 |                        | Nov 2004–Dec 2004 |                        | Dec 2004–May 2009 |                        |  |
|---|-------------------|------------------------|-------------------|------------------------|-------------------|------------------------|-------------------|------------------------|--|
| Morphologic Sand Budget for Short Monitoring Reaches (Mg)     |                   |                        |                   |                        |                   |                        |                   |                        |  |
| R2  | 22,000            | ± 16,000               | 231,000           | ± 16,000               | –189,000          | ± 16,000               |                   |                        |  |
| R3  | –8,000            | ± 8,000                | 14,000            | ± 9,000                | –5,000            | ± 10,000               |                   |                        |  |
| R4  | –9,000            | ± 9,000                | 27,000            | ± 9,000                | –40,000           | ± 10,000               | 71,000            | ± 10,000               |  |
| R5  | –15,000           | ± 19,000               | 19,000            | ± 19,000               | –91,000           | ± 19,000               | 175,000           | ± 20,000               |  |
| R6  | –18,000           | ± 15,000               | 11,000            | ± 15,000               | –68,000           | ± 15,000               | 97,000            | ± 16,000               |  |
| Morphologic Budget Extrapolated to Mass-balance Segments (Mg) |                   |                        |                   |                        |                   |                        |                   |                        |  |
| UMC   | 30,000            | ± 304,000 <sup>a</sup> | 1,525,000         | ± 310,000 <sup>a</sup> | –1,273,000        | ± 335,000 <sup>a</sup> |                   |                        |  |
| LMC   | –204,000          | ± 318,000 <sup>a</sup> | 240,000           | ± 319,000 <sup>a</sup> | –939,000          | ± 333,000 <sup>a</sup> | 1,578,000         | ± 345,000 <sup>a</sup> |  |
| Flux-based Sand Budget for Mass-balance Segments (Mg)         |                   |                        |                   |                        |                   |                        |                   |                        |  |
| UMC   | –72,000           | ± 89,000               | 441,000           | ± 104,000              | –453,000          | ± 23,000               | 693,000           | ± 702,000              |  |
| LMC   | –313,000          | ± 82,000               | 79,000            | ± 44,000               | –172,000          | ± 54,000               | 218,000           | ± 371,000              |  |

LMC, lower Marble Canyon; UMC, upper Marble Canyon.

<sup>a</sup>The uncertainty applied to the extrapolated budgets assumes zero extrapolation error and, therefore, likely underestimates total uncertainty.

change in the flux-based mass balance for each corresponding time period, within uncertainty limits.

[39] The interval between May 2002 and May 2004 was a 2 year period with no dam-released floods, very little tributary sand inputs, and slightly declining or stable sand budgets (Table 3). Substantial Paria River sand inputs only occurred during one flood in August 2003, which caused a significant increase in the flux-based sand mass balance for upper Marble Canyon (Figure 2). The flux-based sand budget indicated that the mass balance was likely negative in upper Marble Canyon and significantly negative in lower Marble Canyon during the 2 year period (Figure 2). The morphologic budget for the period indicates net deposition in R2 and net erosion in the other short monitoring reaches; however, many of these changes were smaller than the uncertainty bounds. The morphologic budgets extrapolated from the short monitoring reaches to the mass-balance segments agree with the flux-based measurements within the uncertainty bounds.

[40] For the 6 month period between May 2004 and November 2004, during which there were no dam-released floods and large tributary sand inputs, both budgeting methods showed significant sand accumulation. Three Paria River floods resulted in sand accumulation throughout Marble Canyon during this interval, as shown in the flux-based mass balance (Figure 2). The repeat surveys also indicated that sand storage increased in all monitoring reaches during this period, and the accumulation was greatest in R2, immediately downstream from the Paria River confluence. In this case, the budget based on extrapolated morphologic measurements exceeded the flux-based mass balance by about a factor of 3 in each of the mass-balance segments (Table 3). This indicates that the magnitude of sand storage changes measured in the short monitoring reaches was not representative of the sand storage changes throughout the longer mass-balance segments. A portion of the disagreement may be explained by reach location. R2 is immediately downstream from the Paria River and more sand accumulated here than in R3. If R2 was excluded from the extrapolated budget, the extrapolated storage change and the flux-based mass balance would agree within uncertainty limits. There is no corresponding explanation for the difference between the extrapolated storage change and the flux-based mass balance for lower Marble Canyon, however.

[41] During the short period from November 2004 to December 2004, when there was one dam-released flood and no additional sand inputs, the morphologic and flux-based budgets both showed significant sand loss. This interval included a 1200 m<sup>3</sup>/s controlled flood that lasted approximately 2 days. This event resulted in the deposition of sand along the channel margins in upper and lower Marble Canyon [Topping *et al.*, 2006a; Schmidt and Grams, 2011], but a net export of sand from both mass-balance segments (Figure 2). There was also net erosion beyond the range of uncertainty in four out of the five short monitoring reaches (Table 3). Yet, when the morphologic budget is extrapolated from the short monitoring reaches to the scale of the mass-balance segments, the magnitude of erosion is greatly overestimated compared with the flux measurements.

[42] Both the morphologic and flux-based budgets indicated sand accumulation for the 4.5 year period between December 2004 and May 2009. However, in the flux-based budget, that accumulation was less than the uncertainty. In the morphologic

budgets for the short monitoring reaches, the accumulation exceeded the uncertainty estimates (Table 3). During this time period, there were several Paria River floods and a controlled flood in March 2008 (Figure 2). The lower Marble Canyon flux-based mass balance indicated progressive sand accumulation up to the date of the controlled flood, net sand erosion during the flood, and no significant sand accumulation or depletion between the controlled flood and the 2009 survey. By the end of the budget period in 2009, the uncertainties in the flux-based budget were larger than the estimated sand storage changes, because this period involved a large cumulative flux of sand. The sand storage changes in the short monitoring reaches all exceeded uncertainty.

[43] As in most of the other budgeting periods described above, the 2004–2009 sand storage change extrapolated from the short monitoring reach to the entire mass-balance segment agrees in sign with the flux-based mass balance but appears to largely overestimate the magnitude of storage change. These observations illustrate an important difference between the sand budgeting methods. The accumulation of uncertainty in the flux-based budget limits the ability to confidently determine net storage change over long time periods that involve large cumulative fluxes of sediment. This accumulation of uncertainty does not affect the morphologic budgets. The weakness of the morphologic budgets is the extrapolation from the measured to unmeasured areas. The lack of agreement between the extrapolated morphologic budget and the flux-based budget suggests that unobserved morphologic changes in the larger part of the long mass-balance segment outside of the short monitoring reaches had to be very different from the morphologic changes observed within the short reaches. Explanations for this result are discussed below.

### 5.3. Spatial Variability of Changes in Sediment Storage

[44] The observed disagreement between the flux-based sand budget and the extrapolated morphologic budget most likely arises from a sampling scheme that failed to represent the full range of spatial variability in sand storage dynamics controlled by local hydraulics. Although the uncertainties in the flux-based budgets are very large for some time intervals, the difference between those budgets and the extrapolated morphologic budgets is often much larger than that uncertainty range. Thus, the extrapolation from the measured to unmeasured areas, which was based only on reach length and width, is the likely source of the disagreement. In the extrapolation, it was assumed that the short monitoring reaches have the same frequency of sand storage locations and that their hydraulic-controlled behavior is representative of storage locations outside the short monitoring reaches. While we do not know what changes occurred outside the short monitoring reaches, inspection of the spatial variability of change within the short monitoring reaches is revealing.

[45] Eddies are one of the major foci of sand storage monitoring in Grand Canyon, because most of the emergent sandbars of interest are within these zones of recirculating flow [Schmidt, 1990]. Additionally, Hazel *et al.* [2006] estimated that between 51 and 94% of changes in sand storage occurred within EDZs, which account for less than one third of the area of the channel in the mapped reaches. That estimate was based on sand storage changes measured

for individual EDZs and the adjacent channel and was based on the estimation that 11% of the bed outside of EDZs was covered by sand [Hazel *et al.*, 2006]. Maps depicting the spatial distribution of sand storage changes observed in this study (Figure 5) illustrate that eddies are highly active storage environments. Whether the interval is dominated by erosion or deposition, changes on the order of 1 m or more are concentrated in EDZs, whereas large areas of the channel experience little or no change. In some intervals, changes in EDZs account for up to 75% of the measured deposition (Table 4). On average, about 50% of the changes

in sand storage occur within EDZs, as suggested by the lower bound of the estimate by Hazel *et al.* [2006]. However, substantial changes in sand storage occur in other locations as well. During periods of sand accumulation, e.g., May to November 2004 in R2, as little as 24% of the deposition occurred in EDZs. This indicates that although the sand storage changes are disproportionately concentrated in EDZs, the changes in the channel outside EDZs are also significant. The sand storage changes outside EDZs are not evenly distributed but are typically greatest in the channel adjacent to the eddy (Figure 5). These sections of channel

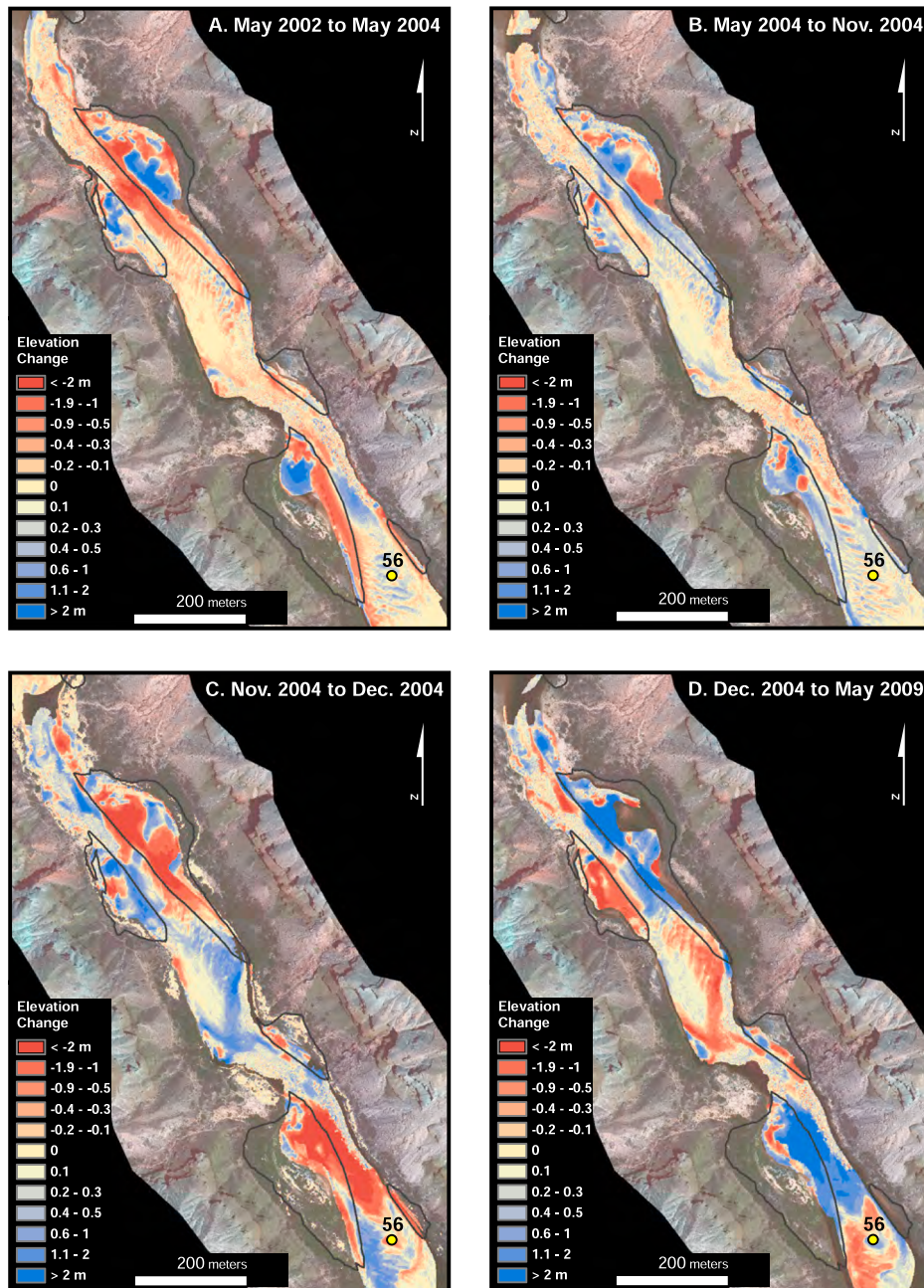


**Figure 5.** Maps showing erosion and deposition for a portion of R6 upstream from RM 56. The eddy deposition zones (EDZs) are outlined by the gray polygons. (a) May 2002 to May 2004. (b) May 2004 to November 2004. (c) November 2004 to December 2004. (d) December 2004 to May 2009. Streamflow direction is from north to south.

**Table 4.** Proportion of Change in Storage Within Eddy Depositional Zones (EDZs)

| Period                      | Reach                     | Erosion in EDZs, % | Deposition in EDZs, % | Activity <sup>a</sup> in EDZs, % |
|-----------------------------|---------------------------|--------------------|-----------------------|----------------------------------|
| May 2002–May 2004           | R2                        | 41                 | 40                    | 41                               |
|                             | R3                        | 56                 | 56                    | 56                               |
|                             | R4                        | 44                 | 41                    | 43                               |
|                             | R5                        | 35                 | 60                    | 46                               |
|                             | R6                        | 52                 | 75                    | 61                               |
|                             | Average for time interval |                    | 46                    | 54                               |
| May 2004–Nov 2004           | R2                        | 71                 | 24                    | 26                               |
|                             | R3                        | 61                 | 53                    | 56                               |
|                             | R4                        | 55                 | 35                    | 40                               |
|                             | R5                        | 43                 | 58                    | 52                               |
|                             | R6                        | 69                 | 51                    | 59                               |
|                             | Average for time interval |                    | 60                    | 44                               |
| Nov 2004–Dec 2004           | R2                        | 24                 | 53                    | 28                               |
|                             | R3                        | 75                 | 73                    | 74                               |
|                             | R4                        | 38                 | 36                    | 37                               |
|                             | R5                        | 52                 | 27                    | 44                               |
|                             | R6                        | 63                 | 36                    | 54                               |
|                             | Average for time interval |                    | 50                    | 45                               |
| Dec 2004–May 2009           | R4                        | 36                 | 35                    | 35                               |
|                             | R5                        | 37                 | 43                    | 42                               |
|                             | R6                        | 45                 | 64                    | 60                               |
| Average for time interval   |                           | 39                 | 47                    | 45                               |
| Average among all intervals |                           | 50                 | 48                    | 47                               |

<sup>a</sup>Sum of erosion and deposition.

include the plunge pool or scour hole that typically exists downstream from rapids and the pool exit slope at the downstream end of the plunge pool.

[46] The simple classification of the channel into units categorized as pools and units categorized as rapids or riffles demonstrates that changes in sand storage are, in fact, much greater in the pools, which include EDZs and the adjacent channel. On average, 81% of the changes in sand storage occurred in pools with the remainder occurring in riffles. While sand storage changes are clearly concentrated in the

pools, there is large variability in the magnitude and direction of change among the pools in any given reach (Figure 6). For example, in R5 the deepest pool experienced the greatest scour between November and December 2004. However, during this same interval, other deep pools had much less scour and some filled. There was no correlation between pool depth and the magnitude of storage change (Figure 7). In fact, sand storage changes in just a few of the most active pools are large relative to the total flux-based mass balance for a given segment. For example, in the most active 100 m channel units

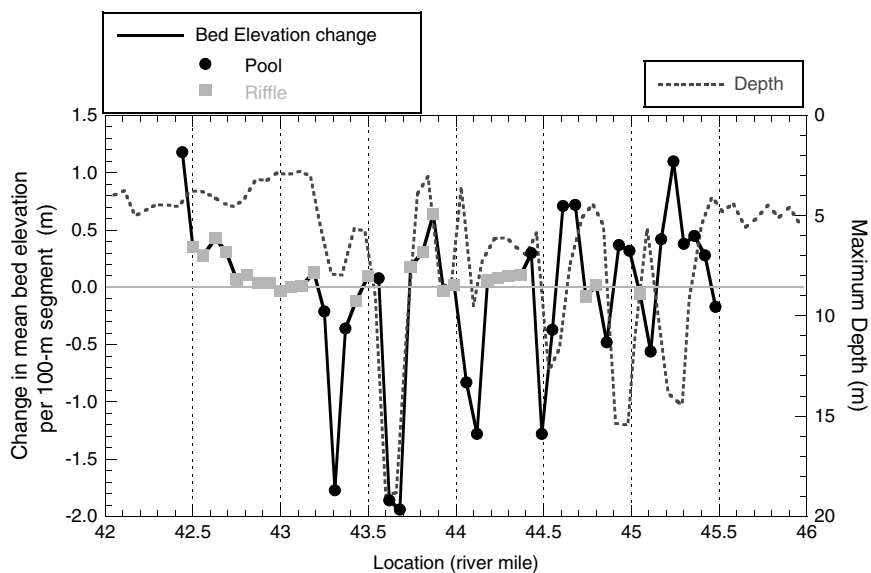


**Figure 6.** Plot showing maximum depth and change in mean bed elevation for R5 between November and December 2004 per 100 m channel unit. Change in mean bed elevation is calculated as the net volume change for each 100 m channel unit divided by the area mapped in that 100 m unit. The 100 m units that are in riffles are shown by the squares, and the units in pools are shown by the circles. The largest volume changes all occur within pools, but not all deep pools experienced large changes in sediment storage volume.

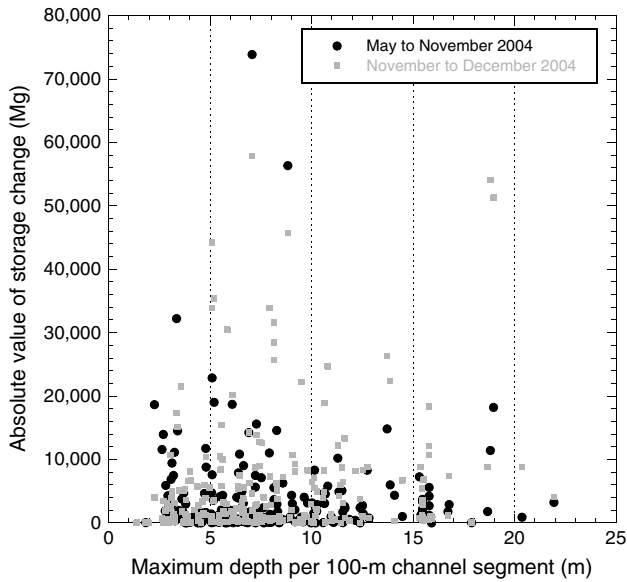


**Figure 7.** Plot showing sediment storage change per 100 m channel unit as a function of maximum depth in the same 100 m channel units for changes occurring between May 2004 and November 2004 (black circles) and between November 2004 and December 2004 (gray squares) in all five short monitoring reaches.

in R5, changes in sand storage typically exceed the average change for the encompassing 50 km mass-balance segment by a factor of 20 or more (Figure 8). In some cases, the sand storage change in individual 100 m channel units exceeds the

segment-average change by more than a factor of 100. This illustrates the complex relation between local changes in sand storage and segment-scale mass balance.

[47] Variability in the response of eddy-deposited sandbars has been observed following each of the controlled floods released from Glen Canyon Dam [Hazel *et al.*, 1999; Schmidt *et al.*, 1999; Hazel *et al.*, 2010]. Because these observations were based on monitoring of individual sites spaced several kilometers apart, it was not clear whether that variability resulted from the small sample size, reach-scale differences in sand supply, or differences in the hydraulic characteristics affecting patterns of erosion and deposition. The repeat surveys of short reaches presented here show that the local variability within an individual reach is at least as large as the variability between reaches (Figure 8). This suggests that local hydraulics, as indicated by the physical scaling analysis presented in section 1, and not reach-scale differences in sand supply, are the major cause of response variability.

[48] The influence of hydraulics on sand storage patterns is illustrated by data from selected eddies within the short monitoring reaches that have much longer monitoring records. Between 11 and 22 repeat topographic/bathymetric surveys were conducted at 30 sites in all of Grand Canyon (11 sites in Marble Canyon) between 1992 and 2008 [Hazel *et al.*, 2010]. These surveys used the same methods that were used for monitoring reaches R2–R6 but were limited to single pools, i.e., individual eddies and the immediately adjacent channel. These data illustrate processes of sand redistribution that can only be shown by many observations made across a range of discharges. For each survey, a single discharge was selected to characterize the flow associated with the observed topography. Conceptually, this discharge is considered to

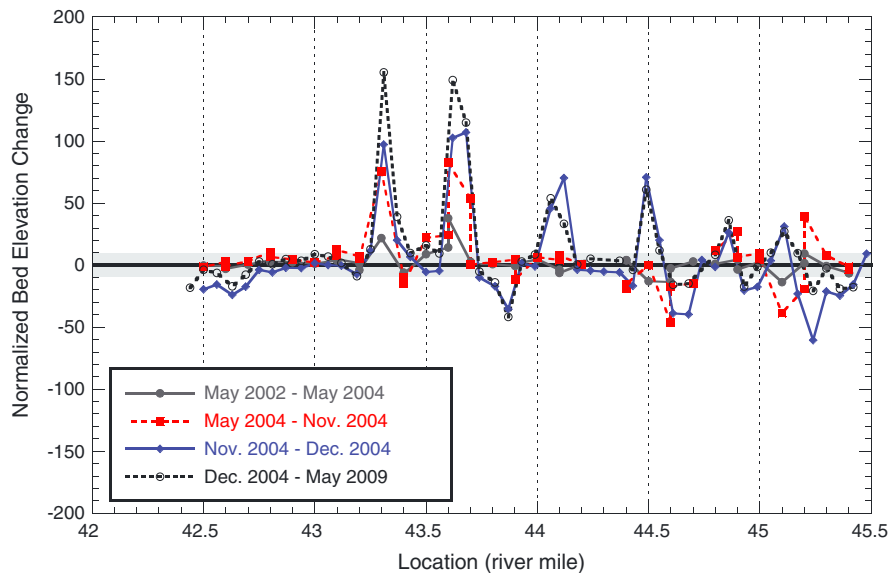


**Figure 8.** Plot showing normalized changes in mean bed elevation by 100 m channel unit in R5 for each morphologic monitoring interval. The changes in mean bed elevation are normalized by the average change in bed elevation associated with the flux-based mass balance for the same time interval. The thick black line indicates the range that is between  $-1$  and  $+1$ ; points that fall on this line depict storage changes that are equal to the reach-average change indicated by the flux-based budget. The shaded region indicates the range between  $-10$  and  $+10$ ; points that fall within this range depict storage changes that are within a factor of 10 of the reach-average change indicated by the flux-based budget. Points falling outside this region depict local changes in storage that exceed the reach-average change by more than a factor of 10.

be the formative discharge for the channel morphology observed at the time of the survey. Daily surveys made during controlled floods indicate that sand deposition occurs relatively rapidly in the first 2 to 3 days of a flood

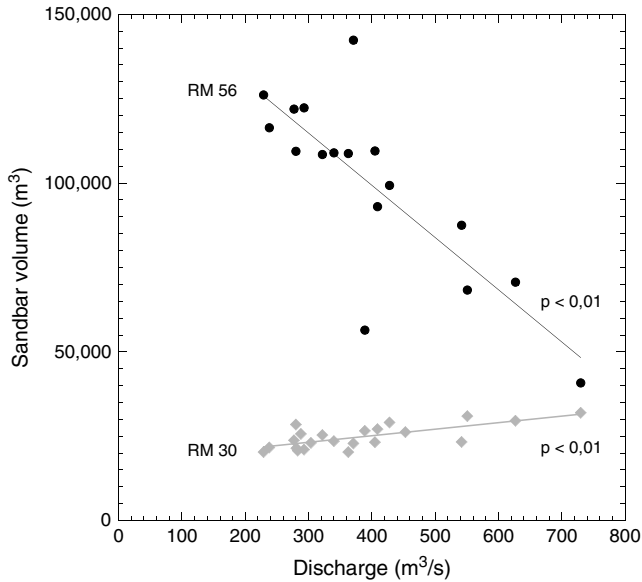


**Figure 9.** Relation between sediment storage volume and formative discharge for two EDZs in Marble Canyon. The sediment storage volume is the volume of sediment above a specified reference elevation (Hazel *et al.*, 2010), and the formative discharge is the mean of daily mean discharges for the 20 days preceding the survey. The positive relation for the EDZ on the west side of the river near RM 30 is shown by the diamonds. The negative relation for the EDZ on the west bank of the river near RM 56 is shown by the circles.

[Andrews *et al.*, 1999; Wright and Kaplinski, 2011]. The adjustment time for lower discharges is not known but is likely to be significantly longer. Regardless, the selection of a formative discharge is relatively insensitive to the assumed adjustment time, because operating regimes tend to be consistent for periods of several weeks (Figure 2). The mean of daily mean discharges for periods between 5 and 30 days typically differ by less than 5%. We, therefore, chose the mean of the instantaneous discharges for the 20 days preceding a survey as a proxy for the formative discharge.

[49] As expected on the basis of the physical scaling analysis presented in section 1, the majority of the 30 long-term monitoring sites exhibit a significant correlation between formative discharge and sand storage volume. Storage volume is negatively correlated with discharge at 43% of the sites and positively correlated with discharge at 23% of the sites (significant correlation was evaluated with an *F*-test requiring that  $p < 0.15$ ). Discharge and sand storage volume are uncorrelated at 34% of the sites. The trends in these relations indicate that for a given discharge, some sites tend to evacuate sand and maintain a low storage volume while other sites tend to accumulate sand and maintain a relatively large storage volume. Figure 9 illustrates these relations for two sites in Marble Canyon. The site near RM 30 has a positive relation between discharge and sand storage volume, whereas the site near RM 56 has a negative relation. These sites are not separated by any significant tributaries and have similar conditions of sand supply (Figure 2). Yet during the period before the 2004 controlled flood (May to November 2004), when the mass balance demonstrated sand accumulation in that river segment (Figure 2), sand evacuation occurred at the site near RM 30 (Figure 10a), while sand accumulation occurred at the site near RM 56 (Figure 5b). The formative discharge preceding this measurement was relatively low ( $\sim 230 \text{ m}^3/\text{s}$ ), and the response at each site was consistent with

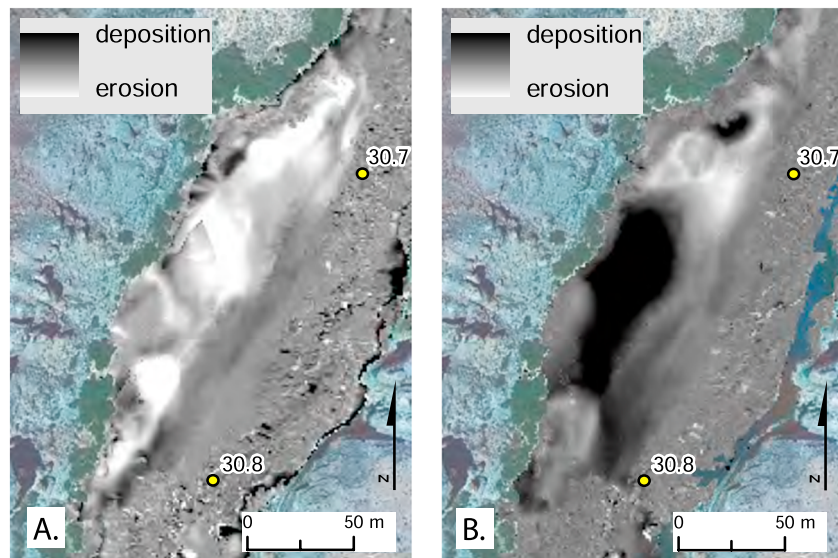


**Figure 10.** Maps showing erosion and deposition for the EDZ on the west side of the river near RM 30. (a) The interval between May and November 2004 showing erosion in the EDZ that is consistent with the response expected for a survey at relatively low discharge for this site (Figure 9, diamonds). (b) The interval between November and December 2004 showing widespread deposition in the EDZ that is consistent with the response expected for a survey at relatively high discharge for this site.

its respective discharge-sand storage relation (Figure 9). Despite the positive mass balance, sand accumulation only occurred at RM 56 where accumulation is expected at relatively low formative discharge. In the next survey interval (November to December 2004), which included a controlled flood and a relatively high formative discharge ( $\sim 410 \text{ m}^3/\text{s}$ ), the site near RM 30 accumulated sand (Figure 10b) while the site near RM 56 lost sand (Figure 5c). These responses are again consistent with the response expected based on the relations in Figure 9.

[50] These results demonstrate empirically that at the scale of individual pools, and as expected on the basis of equation (10), local hydraulics can exert a stronger control on sand storage changes than does the segment-scale sand mass balance. These findings are consistent with those of *Colby* [1964] and *Topping et al.* [2000b]. These previous studies did not, however, quantify either the magnitude or spatial extent of local sediment storage changes, because they lacked reach-scale morphologic measurements. The morphologic sand budgets developed for this study show that for short reaches composed of several individual pools, changes in sand storage will depend on the particular combination of individual sites and how these sites independently respond to changes in discharge and changes in sand supply. The results from repeat maps of the short monitoring reaches indicate that these reaches, each of which includes between 11 and 25 large EDZs, do not include a large enough sample of EDZs such that the sand storage response matches the mass balance for a much longer reach. While there must exist a spatial scale at which the discharge-dependent sand redistribution is balanced, these findings suggest that a sample consisting of 20% of the reach of interest is inadequate to develop a morphologic sediment budget.

## 6. Discussion

[51] Repeat measurements of channel morphology are often made to study the dynamics of specific channel features, evaluate local channel stability, or monitor following river restoration projects. Repeat measurements of channel morphology are also used to make inferences about a river's sediment supply regime and, ultimately, whether the river is in an aggradational, degradational, or approximate equilibrium state. It was with the latter objective that *Leopold and Maddock* [1953] examined changes in channel cross-section form in relation to sediment supply at selected stream gaging stations and concluded that channel scour and fill were related to variations in sediment supply. In contrast, *Colby* [1964] and *Topping et al.* [2000b] provided evidence that local hydraulics, not sediment supply, controlled local channel response during the course of one season's flood. Although changes in sediment supply could modify, and in rare cases offset, channel response during a flood, *Topping et al.* [2000b] showed that as long as the upstream sediment supply was not zero, local hydraulics were much more important in controlling channel response during a flood. In other words, hydraulics are expected to determine the direction of response while supply is expected to either amplify or dampen the response. These studies and others in a variety of channel types [e.g., *Andrews*, 1979; *Lane et al.*, 1996; *Powell et al.*, 2006] have shown that in order to establish a connection between channel morphologic change and sediment supply,

one must study a reach that is sufficiently long to be representative of average channel response and overcome the variability caused by local hydraulics.

[52] While the processes that cause local hydraulics to dominate local channel response have been known for decades, the spatial extent of these processes has not been defined. More importantly, the net influence of local processes on the reach-scale sediment mass balance had not been evaluated. In this study, we show that local changes in sediment (sand) storage on the Colorado River in Marble Canyon involve entire pools that consist of a recirculating eddy and the adjacent channel. In addition, we show that the magnitude of these changes is often large relative to the total sand mass balance for a much longer reach. Thus, a sediment budget that is estimated based on morphologic measurements that are collected as a subsample of a longer mass-balance reach can be significantly skewed or perhaps made invalid by the inclusion or exclusion of a small percentage of sites that have large morphologic changes that are largely driven by local hydraulics.

[53] Changes at the scale of the short monitoring reaches that are not consistent with the long-reach sand mass balance could either result from local hydraulics or variations in sand supply within the 50 km mass-balance segment. It is possible, for example, that sand inputs contributed by the Paria River move downstream as a sediment pulse similar to that described for bedload dominated systems [e.g., *Gilbert*, 1917; *Madej and Ozaki*, 1996]. In this case, one might expect to see large differences in sand storage changes between reaches that are 10s of kilometers apart, but similarity in response within the short monitoring reaches. The monitoring data for this study period in Marble Canyon suggest the opposite. The within-reach variability in sand storage change is, in fact, greater than the variability between reaches. Within each short monitoring reach, there are pools that are consistently stable, pools that consistently evacuate sand, and pools that consistently accumulate sand during each time interval (Figure 5). Nevertheless, for any given time interval, the direction of the change in storage is consistent among the short monitoring reaches and tends to agree with the segment-scale sand mass balance. This is another indication that variability is driven by local hydraulics and not sand supply conditions, such as would be the case with a downstream migrating sediment pulse. We also interpret this to mean that the sample size represented by each short monitoring reach was sufficiently large to correctly predict the sign of the systemwide sand budget. That is, we can be reasonably confident that the direction of change in storage indicated by the short monitoring reaches is indicative of the trend in mass balance for the encompassing mass-balance segment. However, the magnitude of the imbalance predicted from an extrapolation from the short monitoring reaches to the longer segments is uncertain.

[54] At the outset of this monitoring effort, it was anticipated that the selected reaches included a representative sample of storage environments such that they would provide a reasonable measure of sand storage changes for the mass-balance segments. The short monitoring reaches are between 20 and 60 channel widths in length and four out of the five include more than 20 large EDZs. Prior to this study, monitoring of sand storage change in Marble Canyon included repeat surveys of channel cross-sections between

1992 and 1999 [Flynn and Hornewer, 2003] and periodic measurements at a selection of eddy sandbars [Hazel et al., 2006]. Both the cross-section measurements and the sandbar surveys showed spatial variability in  $\Delta S$ , but the limited spatial resolution of the measurements prevented complete description of that variability. The data collected for this study provide, for the first time, a comprehensive portrait of sand storage change and its variability for more than a single debris fan-eddy complex. Even though it is somewhat discouraging that the short monitoring reaches are not representative of the magnitude of changes in sand storage over longer reaches, the measurements provide valuable insight that can be used in the design of future monitoring efforts.

[55] These findings suggest that a robust estimate of sediment storage change based on repeat morphologic measurements requires either monitoring the entire reach of interest, random sampling of a known population of storage locations, or stratified sampling based on predictive understanding of local variability caused by local hydraulics. To implement random sampling would require determination of the number of important sediment storage locations and estimation of the variance of storage changes. For example, the data collected in this study could be used to estimate the variance of sand storage change. If these quantities are not known, it may be necessary to follow the first approach and measure the entire segment. The third approach involves stratified sampling of storage locations based on their known pattern of behavior. For example, this approach could be based on discharge-sediment storage relations like those shown in Figure 9. This approach requires knowledge of not only the number of storage locations, but also predictive understanding of their response pattern. It may, however, not be possible to achieve the necessary predictive understanding without first mapping channel changes comprehensively for the reach of interest for some period of time. Only once local dynamics are understood and predictable would it be possible to devise a stratified sampling scheme.

[56] The description of sand storage changes dominated by the hydraulic-controlled behavior of eddies and pools in Grand Canyon presented here is only one example of this process. Certainly, these processes are equally important in other debris-fan dominated rivers [Schmidt et al., 1995; Schmidt and Rubin, 1995]. While we believe that similar processes occur in all rivers, the relative importance of hydraulic-controlled sediment redistribution will vary greatly depending on the type and distribution of sediment storage locations. In general, hydraulic-controlled sediment redistribution is likely to be most important in rivers with distinct sediment storage locations that are determined by channel geometry. In contrast, low-gradient alluvial rivers, which have wide and relatively uniform flood plains, likely exhibit a weaker influence by local hydraulics. Thus, sampling of morphologic change likely provides a better approximation of the reach-average sediment budget in these settings.

[57] Although the emphasis here has been on local variability in sediment storage change and the influence of local hydraulics, we do not suggest that sediment storage changes are decoupled from sediment supply. The coupling between sediment supply and morphodynamic response is very clear in the physical scaling analysis (equation (10)). Nevertheless, the coupling between sediment supply and the local morphologic response of the bed is not as strong as is the coupling

between local hydraulics and the local morphologic response of the bed. In each of the monitoring intervals, there is a significant and consistent response among the short monitoring reaches that is consistent with the flux-based mass balance. Each reach shows evidence of sand accumulation during periods of positive sand mass balance and evidence of sand evacuation during periods of negative sand mass balance. Moreover, the uncertainty in the computed sand storage change for the short monitoring reaches is smaller than the uncertainty in the flux-based mass balance, except for some of the relatively short intervals between measurements when flux-based uncertainties are lower. While the magnitude of storage change in the long mass-balance reaches cannot be accurately estimated based on measurements from the short monitoring reaches, the short reaches with low uncertainty do support the trend indicated by the flux-based mass balance. For example, in the long interval between December 2004 and May 2009, the flux-based mass balance indicates sand accumulation, but with uncertainty that is larger than the predicted accumulation. The result is an indeterminate prediction of the mass balance (Table 3). However, each of the short monitoring reaches shows sand accumulation with relatively small uncertainty. This lends confidence that the direction of sand storage change that is suggested by the flux-based mass balance is correct.

[58] These findings also have implications for the management of sediment-related resources along the Colorado River in Grand Canyon National Park. The 2002 to 2009 study period included two controlled floods released for the purpose of rebuilding sandbars in EDZs. Schmidt and Grams [2011] reported that each of those floods built sandbars in Marble Canyon. Despite widespread erosion of newly built sandbars following each flood, Schmidt and Grams [2011] also reported that 7 out of 12 sandbars monitored from 1996 to October 2008 experienced a net increase in size during that period. The flux-based sand budgets for upper and lower Marble Canyon and the three morphologic-based budgets for lower Marble Canyon all indicate net increases in sand storage between May 2004 and May 2009. Because of the large uncertainty in these estimates, it is not possible to conclude whether the net increase in storage was slight or substantial. It is clear, however, that the trend in sand storage was not negative, which is encouraging for the rehabilitation of eddy sandbar size in Grand Canyon National Park. This status of the sand budget suggests that it is possible to use repeated controlled floods as a method for sandbar restoration without causing net depletion of sand from storage in the river channel. However, it is also important to recognize that average dam releases in the study period were about 12% lower than average since dam completion. This is consistent with the findings of Wright et al. [2008]. Based on a simple sand routing model, they concluded that progressive sandbar restoration in Grand Canyon may be possible with average or lower annual dam release volumes. The degree to which sandbar restoration goals can be met under average or higher dam releases remains uncertain.

## 7. Conclusions

[59] Flux-based sand budgets derived from measurements of sediment transport were compared with morphologic-based sand budgets derived from measurements of channel morphology for the 100 km Marble Canyon segment of

the Colorado River in Grand Canyon National Park. The flux-based budget was based on a continuous (15 min) record of streamflow and suspended-sand transport, and the morphologic-based budget was based on repeat mapping of five “short” (3–5 km) study reaches. Sand storage trends within the short monitoring reaches were consistent with the trends in flux-based mass balance throughout the 2002 to 2009 study period. Sand was eroded from each study reach during periods when the flux-based budget was negative, and deposition occurred in each reach when the flux-based budget was positive. It was not possible to accurately extrapolate the morphologic measurements beyond the short reaches to estimate the magnitude of sand storage changes for longer segments. Observations of local changes in sand storage demonstrate that the interaction of the flow with local channel geometry exerts a much stronger control on morphodynamic response than do changes in the upstream sand supply. Changes in the upstream supply of sand amplify or dampen bed responses, but local hydraulics dominate the morphodynamic response. Thus, accurate sediment budgets constructed from morphologic measurements must incorporate the effect of local hydraulics in a sampling design or must avoid extrapolation altogether.

[60] Both the flux- and morphologic-based sand budgets indicate that there was no significant net decrease in the amount of sand stored in the river channel in Marble Canyon at the end of the 7 year study period, which was a period of below-average dam releases. While it is possible that sand storage increased, uncertainty associated with the accumulation of potential bias in the flux-based budget and extrapolation error in the morphologic budget prevents determining the magnitude of significant increase.

[61] **Acknowledgments.** The data analyzed and discussed in this report were collected and processed over many years by the dedicated efforts of many field technicians, river guides, and volunteers. We especially acknowledge Robert Ross, Robert Tusso, Tom Gushue, Nathan Schott, and Mike Breedlove for the assistance they provided with data processing and analysis. Mapping long reaches of the Colorado River in Grand Canyon is made possible with the geodetic control network maintained by Keith Kohl, with assistance from Aaron Borling and Michael Dennis. Helpful comments from David Gaeuman, John Buffington, Ted Melis, and Chris Magirl helped improve the manuscript. This work was funded by the Glen Canyon Dam Adaptive Management Program administered by the U.S. Bureau of Reclamation. Any use of trade, product, or firm names is for descriptive purposes only and does not imply endorsement by the U.S. Government.

## Notation

|                      |   |
|----------------------|---|
| $A$                  | area of interest for sediment budget computation, $m^2$                     |
| $A_c$                | area of grid cell in DEM, $m^2$   |
| $A_s$                | fractional amount of suspendable bed material on bed surface, dimensionless |
| $C_s$                | suspended-sediment concentration, dimensionless                             |
| $D_b$                | median size of suspendable bed material, m                                  |
| $F_{s\text{rough}}$  | proportion of rough surface that is sand, dimensionless                     |
| $F_{s\text{smooth}}$ | proportion of smooth surface that is sand, dimensionless                    |
| $h$                  | flow depth, m   |
| $I$                  | sediment influx, Mg   |
| $I'$                 | uncertainty in sediment influx, Mg  |
| $O$                  | sediment flux, Mg   |

|                            |   |
|----------------------------|---|
| $O'$                       | uncertainty in sediment efflux, Mg  |
| $q_s$                      | sediment flux per unit width, $m^2/s$   |
| $Q_s$                      | sediment flux, $m^3/s$  |
| $t$                        | time, s   |
| $U$                        | streamflow velocity, m/s  |
| $u_*$                      | shear velocity, m/s   |
| $V_s$                      | volumetric concentration of suspended sediment, dimensionless                 |
| $X$                        | streamwise coordinate, m  |
| $Z_c$                      | elevation of grid cell in DEM, m  |
| $\bar{Z}$                  | spatially averaged elevation, m   |
| $\bar{Z}'$                 | uncertainty in spatially averaged elevation, m                                |
| $\Delta S$                 | change in sediment storage, Mg  |
| $\Delta S_m$               | change in sediment storage based on morphologic difference, Mg                |
| $\Delta S'_m$              | uncertainty in change in sediment storage based on morphologic difference, Mg |
| $\Delta S_f$               | flux-based change in sediment storage, Mg                                     |
| $\Delta S'_f$              | uncertainty in flux-based change in sediment storage, Mg                      |
| $\Delta V_{\text{rough}}$  | fraction of volume change classified as rough, dimensionless                  |
| $\Delta V_{\text{sand}}$   | fraction of volume change that is sand, dimensionless                         |
| $\Delta V_{\text{smooth}}$ | fraction of volume change classified as smooth, dimensionless                 |
| $\eta$                     | bed elevation, m  |
| $\lambda_p$                | bed-sediment porosity, dimensionless  |

## References

- Andrews, E. D. (1979), Hydraulic adjustment of the East Fork River, Wyoming to the supply of sediment, in *Adjustments of the Fluvial System: Proceedings of the Tenth Annual Geomorphology Symposium*, edited by D. D. Rhodes and G. P. Williams, pp. 69–94, Binghamton, New York.
- Andrews, E. D. (1986), Downstream effects of Flaming Gorge Reservoir on the Green River, Colorado and Utah, *Geol. Soc. Am. Bull.*, *97*, 1012–1023.
- Andrews, E. D. (1991), Sediment transport in the Colorado River basin, in *Colorado River Ecology and Dam Management*, edited by G. R. Marzolf, pp. 54–74, National Academy Press, Washington, D.C.
- Andrews, E. D., C. Jonston, J. Schmidt, and M. Gonzales (1999), Topographic evolution of sand bars in Grand Canyon during the experimental flood, in *The 1996 Controlled Flood in Grand Canyon*, *Geophys. Monogr. Ser.*, vol. *110*, edited by R. H. Webb et al., pp. 117–130, AGU, Washington, D. C.
- Brasington, J., B. T. Rumsby, and R. A. Mcvev (2000), Monitoring and modelling morphological change in a braided gravel-bed river using high resolution GPS-based survey, *Earth Surf. Proc. Land.*, *25*, 973–990.
- Brasington, J., J. Langham, and B. Rumsby (2003), Methodological sensitivity of morphometric estimates of coarse fluvial sediment transport, *Geomorphology*, *53*, 299–316, doi:10.1016/S0169-555X(02)00320-3.
- Bridge, J. S., and S. L. Gabel (1992), Flow and sediment dynamics in a low sinuosity, braided river: Calamus River, Nebraska Sandhills, *Sedimentology*, *39*, 125–142.
- Brock, J. C., A. H. Sallenger, W. B. Krabill, R. N. Swift, and C. W. Wright (2001), Recognition of fiducial surfaces in LiDAR surveys of coastal topography, *Photogramm. Eng. Rem. S.*, *67*, 1245–1258.
- Brooks, N. H. (1958), Mechanics of streams with movable beds of fine sand, *Trans. Am. Soc. Civ. Eng.*, *123*, 526–594.
- Colby, B. R. (1964), Scour and fill in sand-bed streams, *U.S. Geol. Surv. Prof. Pap.* *462-D*, 39 pp.
- Curry, C. W., R. H. Bennett, M. H. Hulbert, K. J. Curry, and R. W. Faas (2004), Comparative study of sand porosity and a technique for determining porosity of undisturbed marine sediment, *Mar. Georesour. Geotec.*, *22*(4), 231–252, doi:10.1080/10641190490900844.
- Dolan, R., A. Howard, and D. Trimble (1978), Structural control of the rapids and pools of the Colorado River in the Grand Canyon, *Science*, *202*, 629–631.

- Doyle, M. W., E. H. Stanley, and J. M. Harbor (2003), Channel adjustments following two dam removals in Wisconsin, *Water Resour. Res.*, 39(1), doi:10.1029/2002WR001714, 2003.
- Edwards, T. K., and G. D. Glysson (1999), Field methods for measurement of fluvial sediment, in U.S. Geol. Surv. Techniques and Methods, Book 3, Chapter C2, 89 p.
- Erwin, S. O., J. C. Schmidt, J. M. Wheaton, and P. R. Wilcock (2012), Closing a sediment budget for a reconfigured reach of the Provo River, Utah, United States, *Water Resour. Res.*, 48, W10512, doi:10.1029/2011WR011035.
- Flynn, M. E., and N. J. Hornewer (2003), Variations in sand storage measured at monumented cross sections in the Colorado River between Glen Canyon Dam and Lava Falls Rapid, northern Arizona, 1992–99, *U.S. Geol. Surv. Water Resour. Invest. Rep. 03-4104*, 39 pp, Tucson.
- Gilbert, G. K. (1917), Hydraulic-mining debris in the Sierra Nevada, *U.S. Geol. Surv. Prof. Pap. 105*, 154.
- Grams, P. E., and J. C. Schmidt (2005), Equilibrium or indeterminate? Where sediment budgets fail: Sediment mass balance and adjustment of channel form, Green River downstream from Flaming Gorge Dam, Utah and Colorado, *Geomorphology*, 71, 156–181, doi:10.1016/j.geomorph.2004.10.012.
- Grams, P. E., J. C. Schmidt, and D. J. Topping (2007), The rate and pattern of bed incision and bank adjustment on the Colorado River in Glen Canyon downstream from Glen Canyon Dam, 1956–2000, *Geol. Soc. Am. Bull.*, 119(5/6), 556–575.
- Grams, P. E., and P. R. Wilcock (2007), Equilibrium entrainment of fine sediment over a coarse immobile bed, *Water Resour. Res.*, 43(W10420), 14, doi:10.1029/2006WR005129.
- Gray, J. R., and F. J. M. Simoes (2008), Estimating sediment discharge, in *Sedimentation Engineering: Processes, Measurements, Modeling, and Practice*, edited by M. H. Garcia, pp. 1067–1088, Am. Soc. of Civ. Engr.
- Griffiths, R. E., D. J. Topping, T. Andrews, G. E. Bennet, T. A. Sabol, and T. S. Melis (2012), Design and maintenance of a network for collecting high-resolution suspended-sediment data at remote locations on rivers, with examples from the Colorado River, U.S. Geol. Surv. Techniques and Methods, Book 8, chapter C2, p. 44.
- Hazel, J. E., M. Kaplinski, R. Parnell, M. Manone, and A. Dale (1999), Topographic and bathymetric changes at thirty-three long-term study sites, in *The 1996 Controlled Flood in Grand Canyon*, Geophys. Monogr. Ser., vol. 110, edited by R. H. Webb et al., pp. 161–184, AGU, Washington, D. C.
- Hazel, J. E., D. J. Topping, J. C. Schmidt, and M. Kaplinski (2006), Influence of a dam on fine-sediment storage in a canyon river, *J. Geophys. Res.*, 111(F01025), doi:10.1029/2004JF000193.
- Hazel, J. E., Jr., M. Kaplinski, R. A. Parnell, K. Kohl, and J. C. Schmidt (2008), Monitoring fine-grained sediment in the Colorado River Ecosystem, Arizona—Control network and conventional survey techniques, *U. S. Geol. Surv. Open-file Rep. 2008-1276*, 15 pp.
- Hazel, J. E., Jr., P. E. Grams, J. C. Schmidt, and M. Kaplinski (2010), Sand-bar response following the 2008 high-flow experiment on the Colorado River in Marble and Grand Canyons, *U.S. Geol. Surv. Sci. Invest. Rep. 2010-5015*, 52 pp.
- Howard, A., and R. Dolan (1981), Geomorphology of the Colorado River in the Grand Canyon, *J. Geol.*, 89(3), 269–298.
- Jackson, W. L., and R. L. Beschta (1984), Influences of increased sand delivery on the morphology of sand and gravel channels, *Water Resour. Bull.*, 20(4), 527–533.
- Kaplinski, M., J. E. Hazel, R. Parnell, M. Breedlove, K. Kohl, and M. Gonzales (2009), Monitoring fine-sediment volume in the Colorado River Ecosystem, Arizona: Bathymetric survey techniques, *U.S. Geol. Surv. Open-file Rep. 2009-1207*, 41 pp.
- Lane, S. N., K. S. Richards, and J. H. Chandler (1996), Discharge and sediment supply controls on erosion and deposition in a dynamic alluvial channel, *Geomorphology*, 15, 1–15.
- Lane, S. N., and J. H. Chandler (2003), Editorial: The generation of high quality topographic data for hydrology and geomorphology: New data sources, new applications and new problems, *Earth Surf. Proc. Land.*, 28, 229–230, doi:10.1002/esp.479.
- Lane, S. N., R. M. Westaway, and D. M. Hicks (2003), Estimation of erosion and deposition volumes in a large, gravel-bed, braided river using synoptic remote sensing, *Earth Surf. Proc. Land.*, 28, 249–271, doi:10.1002/esp.483.
- Laursen, E. M., S. Ince, and J. Pollack (1976), On sediment transport through the Grand Canyon, paper presented at 3rd Federal Interagency Sedimentation Conference, Sedimentation Committee of the Water Resources Council, Denver, Colo.
- Leopold, L. B., and T. Maddock, Jr. (1953), The hydraulic geometry of stream channels and some physiographic implications, *U.S. Geol. Surv. Prof. Pap. 252*, 56 pp.
- Lisle, T. E. (1982), Effects of aggradation and degradation on riffle-pool morphology in natural gravel channels, northwestern California, *Water Resour. Res.*, 18(6), 1643–1651.
- Lisle, T. E., and S. Hilton (1992), The volume of fine sediment in pools: An index of sediment supply in gravel-bed streams, *Water Resour. Bull.*, 28(2), 371–383.
- Madej, M. A., and V. Ozaki (1996), Channel response to sediment wave propagation and movement, Redwood Creek, California, USA, *Earth Surf. Proc. Land.*, 21, 911–927.
- Magirl, C. S., R. H. Webb, and P. G. Griffiths (2008), Modeling water-surface elevations and virtual shorelines for the Colorado River in Grand Canyon, Arizona, *U.S. Geol. Surv. Sci. Investigations Report 2008-5075*, 32 pp.
- Marron, D. C. (1992), Floodplain storage of mine tailings in the Belle Fourche River system: A sediment budget approach, *Earth Surf. Proc. Land.*, 17, 675–685.
- Merz, J. E., G. B. Pasternack, and J. M. Wheaton (2006), Sediment budget for salmonid spawning habitat rehabilitation in a regulated river, *Geomorphology*, 76, 207–228, doi:10.1016/j.geomorph.2005.11.004.
- Mueller, D. S., and C. R. Wagner (2009), Measuring discharge with acoustic Doppler current profilers from a moving boat, *U.S. Geol. Surv. Techniques and Methods 3A-22*, 72 p.
- Paola, C., and V. R. Voller (2005), A generalized Exner equation for sediment mass balance, *Water Resour. Res.*, 110(F04014), doi:10.1029/2004JF000274, 2005.
- Parker, R. (1988), Uncertainties in defining the suspended sediment budget for large drainage basins, in *Sediment Budgets*, edited, pp. 523–532, IAHS Publication Number 174, Porto Alegre, Brazil.
- Porterfield, G. (1972), Computation of fluvial sediment discharge, U.S. Geol. Surv. Techniques and Methods, Book 3, Chapter C3, 66 p.
- Powell, D. M., R. Brazier, J. Wainwright, A. Parsons, and M. Nichols (2006), Spatial patterns of scour and fill in dryland sand bed streams, *Water Resour. Res.*, 42(W08412), doi:10.1029/2005WR004516, 2006.
- Rantz, S. E., et al. (1982), Measurement and computation of streamflow: Volume 1. Measurement of stage and discharge, *U.S. Geol. Surv. Water Supp. Pap. 2175*, 313 pp.
- Reid, L. M., and T. Dunne (2003), Sediment budgets as an organizing framework in fluvial geomorphology, in *Tools in Fluvial Geomorphology*, edited by G. M. Kondolf and H. Piegay, pp. 463–500, John Wiley & Sons, Ltd., Chichester, UK.
- Rubin, D. M., H. Chezaz, J. N. Harney, D. J. Topping, T. S. Melis, and C. R. Sherwood (2007), Underwater microscope for measuring spatial and temporal changes in bed-sediment grain size, *Sediment. Geol.*, 202, 402–408, doi:10.1016/j.sedgeo.2007.03.020.
- Rubin, D. M., and R. Hunter (1982), Bedform climbing in theory and nature, *Sedimentology*, 29, 121–138.
- Rubin, D. M., and D. J. Topping (2001), Quantifying the relative importance of flow regulation and grain size regulation of suspended sediment transport alpha and tracking changes in grain size of bed sediment beta, *Water Resour. Res.*, 37(1), 133–146.
- Rubin, D. M., and D. J. Topping (2008), Correction to “Quantifying the relative importance of flow regulation and grain size regulation of suspended sediment transport a and tracking changes in grain size of bed sediment b,” *Water Resour. Res.*, 44, W09701, doi:10.1029/2008WR006819.
- Rubin, D. M., G. M. Tate, D. J. Topping, and R. A. Anima (2001), Use of rotating side-scan sonar to measure bedload: Proceedings of the 7th Inter-Agency Sedimentation Conference, v. 1, p. III-139 through III-143.
- Sabol, T. A., and D. J. Topping (2013), Evaluation of intake efficiencies and associated sediment-concentration errors in US D-77 bag-type and US D-96-type depth-integrating suspended-sediment samplers, *U.S. Geol. Surv. Sci. Invest. Rep.*, 2012–5208.
- Schmidt, J. C. (1990), Recirculating flow and sedimentation in the Colorado River in Grand Canyon, Arizona, *J. Geol.*, 98, 709–724.
- Schmidt, J. C., and J. B. Graf (1990), Aggradation and degradation of alluvial sand deposits, 1965 to 1986, Colorado River, Grand Canyon National Park, Arizona, *U.S. Geol. Surv. Prof. Pap. 1493*, 74 p.
- Schmidt, J. C., and P. E. Grams (2011), The high flows—Physical science results, in *Effects of Three High-flow Experiments on the Colorado River Ecosystem Downstream from Glen Canyon Dam*, Arizona, U.S. Geol. Surv. Circular 1366, edited by T. S. Melis, pp. 53–91.
- Schmidt, J. C., P. E. Grams, and R. H. Webb (1995), Comparison of the magnitude of erosion along two large regulated rivers, *Water Resour. Bull.*, 31, 617–631.
- Schmidt, J. C., and D. M. Rubin (1995), Regulated streamflow, fine-grained deposits, and effective discharge in canyons with abundant debris fans, in *Natural and Anthropogenic Influences in Fluvial Geomorphology*, Geophys. Monogr. Ser., vol. 89, edited by J. E. Costa, et al., pp. 177–195, AGU, Washington, D.C.
- Schmidt, J. C., P. E. Grams, and M. F. Leschin (1999), Variation in the magnitude and style of deposition and erosion in three long (8–12 km)

- reaches as determined by photographic analysis, in *The 1996 Controlled Flood in Grand Canyon*, Geophys. Monogr. Ser., vol. 110, edited by R. H. Webb et al., pp. 185–203, AGU, Washington, D. C.
- Schmidt, J. C., D. J. Topping, P. E. Grams, and J. E. Hazel, Jr. (2004), System-wide changes in the distribution of fine sediment in the Colorado River corridor between Glen Canyon Dam and Bright Angel Creek, Arizona, *final report*, 107 pp, U.S. Geol. Surv., Grand Canyon Monitoring and Research Center, Flagstaff, Ariz.
- Sutherland, R. A., and R. B. Bryan (1991), Sediment budgeting: A case study in the Katorin drainage basin, Kenya, *Earth Surf. Proc. Land.*, 16, 383–398.
- Taylor, J. R. (1997), *An Introduction to Error Analysis: The Study of Uncertainties in Physical Measurements*, 2nd ed., University Science Books, Sausalito, California, 327 p.
- Topping, D. J., D. M. Rubin, and L. E. J. Vierra (2000a), Colorado River sediment transport 1. Natural sediment supply limitation and the influence of Glen Canyon Dam, *Water Resour. Res.*, 36(2), 515–542.
- Topping, D. J., D. M. Rubin, J. M. Nelson, P. J. I. Kinzell, and I. C. Corson (2000b), Colorado River sediment transport 2. Systematic bed-elevation and grain-size effects of sand supply limitation, *Water Resour. Res.*, 36(2), 543–570.
- Topping, D. J., J. C. Schmidt, and L. E. Vierra (2003), Computation and analysis of the instantaneous-discharge record for the Colorado River at Lees Ferry, Arizona—May 8, 1921, through September 30, 2000, *U.S. Geol. Surv. Prof. Pap.* 1677, 118 pp.
- Topping, D. J., D. M. Rubin, J. C. Schmidt, J. E. Hazel, Jr., T. S. Melis, S. A. Wright, M. Kaplinski, A. E. Draut, and M. J. Breedlove (2006a), Comparison of sediment-transport and bar-response results from the 1996 and 2004 controlled-flood experiments on the Colorado River in Grand Canyon, paper presented at Federal Interagency Sedimentation Conference, Reno, Nev.
- Topping, D. J., S. A. Wright, T. S. Melis, and D. M. Rubin (2006b), High-resolution monitoring of suspended-sediment concentration and grain size in the Colorado River using laser-diffraction instruments and a three-frequency acoustic system, paper presented at 8th Federal Interagency Sedimentation Conference, Reno, Nev.
- Topping, D. J., S. A. Wright, T. S. Melis, and D. M. Rubin (2007), High-resolution measurements of suspended-sediment concentration and grain size in the Colorado River in Grand Canyon using a multi-frequency acoustic system, paper presented at Tenth International Symposium on River Sedimentation, Moscow, Russia.
- Topping, D. J., D. M. Rubin, P. E. Grams, R. E. Griffiths, T. A. Sabol, N. Voichick, R. B. Tusso, K. M. Vanaman, and R. R. McDonald (2010a), Sediment transport during three controlled-flood experiments on the Colorado River downstream from Glen Canyon Dam, with implications for eddy-sandbar deposition in Grand Canyon National Park, *U.S. Geol. Surv. Open-file Rep.* 2010-1128, 111 pp.
- Topping, D. J., S. A. Wright, R. E. Griffiths, T. S. Melis, D. M. Rubin, and T. A. Sabol (2010b), High-resolution measurements of suspended-sediment concentration and grain size in the Colorado River in Grand Canyon using a multi-frequency acoustic system, paper presented at Hydrology and sedimentation for a changing future; existing and emerging issues (Joint Federal Interagency Conference 2010—Federal Interagency Hydrologic Modeling, 4th, and Federal Interagency Sedimentation, 9th), Las Vegas, Nev.
- Trimble, S. W. (1983), A sediment budget for Coon Creek Basin in the Driftless Area, Wisconsin, 1854–1977, *Am. J. Sci.*, 283, 454–474.
- U.S. Department of the Interior (1995), Final environmental impact statement: Operation of Glen Canyon Dam, Colorado River Storage Project, Coconino County, Arizona, 337 pp, Bureau of Reclamation, Salt Lake City, Utah.
- Walling, D. E., P. N. Owens, and G. J. L. Leeks (1998), The role of channel and floodplain storage in the suspended sediment budget of the River Ouse, Yorkshire, UK, *Geomorphology*, 22(3–4), 225–242.
- Webb, R. H., P. T. Pringle, and G. R. Rink (1989), Debris flows from tributaries of the Colorado River, Grand Canyon National Park, Arizona, *U.S. Geol. Surv. Prof. Pap.* 1492, 39 pp.
- Wheaton, J. M., J. Brasington, S. E. Darby, and D. A. Sear (2010), Accounting for uncertainty in DEMs from repeat topographic surveys: Improved sediment budgets, *Earth Surf. Proc. Land.*, 35, 136–156, doi:10.1002/esp.1886.
- Woodhouse, C. A., S. T. Gray, and D. M. Meko (2006), Updated streamflow reconstructions for the Upper Colorado River Basin, *Water Resour. Res.*, 42(W05415), doi:10.1029/2005WR004455, 2006.
- Wright, S. A., J. C. Schmidt, T. S. Melis, D. J. Topping, and D. M. Rubin (2008), Is there enough sand? Evaluating the fate of Grand Canyon sandbars, *GSA Today*, 18(8), doi:10.1130/GSATG12A.1.
- Wright, S. A., D. J. Topping, D. M. Rubin, and T. S. Melis (2010a), An approach for modeling sediment budgets in supply-limited rivers, *Water Resour. Res.*, 46(W10538), 1–18, doi:10.1029/2009WR008600.
- Wright, S. A., D. J. Topping, and C. A. Williams (2010b), Discriminating silt-and-clay from suspended-sand in rivers using side-looking acoustic profilers, paper presented at Hydrology and sedimentation for a changing future; existing and emerging issues (Joint Federal Interagency Conference 2010—4th Federal Interagency Hydrologic Modeling and 9th Federal Interagency Sedimentation), Las Vegas, Nev.
- Wright, S. A., and M. Kaplinski (2011), Flow structures and sandbar dynamics in a canyon river during a controlled flood, Colorado River, Arizona, *Water Resour. Res.*, 116(F01019), doi:10.1029/2009JF001442, 2011.
- Wright, S. A., and T. A. Kennedy (2011), Science-based strategies for future high-flow experiments at Glen Canyon Dam, in *Effects of Three High-flow Experiments on the Colorado River Ecosystem Downstream from Glen Canyon Dam, Arizona*, U.S. Geol. Surv. Circular 1366, edited by T. S. Melis, pp. 127–147.